



# UNIVERSITA' DEGLI STUDI DI VERONA

*DEPARTMENT OF*

Neurosciences, Biomedicine and Movement Sciences

*GRADUATE SCHOOL OF*

Life and Health Sciences

*DOCTORAL PROGRAM IN*

Biomolecular Medicine (Curriculum Biochemistry)

*WITH THE FINANCIAL CONTRIBUTION OF*

CariVerona Foundation, which funded this PhD fellowship

XXXIV cycle / 2018-2021

TITLE OF THE DOCTORAL THESIS

**NOVEL POTENTIAL TREATMENTS IN THE CHALLENGING SCENARIO OF  
DRUG RESISTANCE IN PANCREATIC DUCTAL ADENOCARCINOMA**

S.S.D. BIO/10 BIOCHIMICA

Coordinator

and Tutor: Prof. DONADELLI MASSIMO



---

Doctoral Student: MASETTO FRANCESCA

---

Quest'opera è stata rilasciata con licenza Creative Commons Attribuzione – non commerciale  
Non opere derivate 3.0 Italia . Per leggere una copia della licenza visita il sito web:

<http://creativecommons.org/licenses/by-nc-nd/3.0/it/>

-  **Attribuzione** Devi riconoscere una menzione di paternità adeguata, fornire un link alla licenza e indicare se sono state effettuate delle modifiche. Puoi fare ciò in qualsiasi maniera ragionevole possibile, ma non con modalità tali da suggerire che il licenziante avalli te o il tuo utilizzo del materiale.
-  **NonCommerciale** Non puoi usare il materiale per scopi commerciali.

**Non opere derivate** —Se remixi, trasformi il materiale o ti basi su di esso, non puoi distribuire il materiale così modificato.

NOVEL POTENTIAL TREATMENTS IN THE CHALLENGING SCENARIO OF DRUG RESISTANCE IN PANCREATIC DUCTAL  
ADENOCARCINOMA

Francesca Masetto  
Tesi di Dottorato  
Verona, 8 Marzo 2022  
ISBN \_\_\_\_\_



## 1. SOMMARIO

Secondo la previsione del Global Cancer Observatory (GCO), una piattaforma web interattiva che presenta statistiche globali sul cancro, l'adenocarcinoma duttale pancreatico (PDAC) è destinato a salire al secondo posto come causa di morte nelle società occidentali entro il prossimo decennio<sup>1</sup>. Ad oggi, la sopravvivenza complessiva dei pazienti a 5 anni dalla diagnosi è solo del 6%, e 25% nei pazienti sottoposti a resezione chirurgica, che però rappresentano soltanto il 15% dei casi totali. I dati enfatizzano la necessità di trovare dei nuovi trattamenti farmacologici efficaci. Gli approcci terapeutici correnti hanno infatti dei grandi limiti: come la chemioresistenza, sia innata che acquista a seguito del trattamento, la mancanza di biomarcatori per target therapy che predicano la risposta del paziente alla terapia, e la tossicità intrinseca dei chemioterapici che causa diversi effetti collaterali.

Questa tesi contiene tre diversi approcci per superare la chemioresistenza nel PDAC, che resta una delle principali sfide terapeutiche della moderna oncologia.

Nella prima parte abbiamo contrastato i meccanismi di resistenza direttamente coinvolti nel metabolismo del farmaco chemioterapico gemcitabina (GEM). Sono stati sintetizzati sette nuovi pro-farmaci di gemcitabina in grado di rilasciare ossido nitrico (NO-GEMs) all'interno delle cellule, al fine di migliorare l'efficacia della GEM sfruttando gli effetti antitumorali dell'NO. Tra questi, il 5b è stato selezionato come il più efficace. Dopo averlo incapsulato in liposomi, per migliorarne l'ingresso nelle cellule, abbiamo dimostrato che l'NO rilasciato dal 5b causa la nitratura e l'inibizione di attività del trasportatore di efflusso (MRP5). Questo si traduce in un accumulo intracellulare di GEM e in una maggiore morte cellulare apoptotica nelle cellule PDAC resistenti alla GEM, che esprimono MRP5 a livelli più alti delle cellule sensibili alla GEM.

I nostri risultati forniscono una valutazione preclinica dell'uso di pro-farmaci NO-GEM come nuova strategia antitumorale per colpire efficacemente le cellule PDAC resistenti alla GEM.

Nella seconda parte dello studio, abbiamo contrastato il rimodellamento metabolico che le cellule tumorali mettono in atto per adattarsi alle sfide del microambiente e facilitare la loro sopravvivenza, proliferazione e la formazione di metastasi. In particolare, l'enzima monoacil glicerol lipasi (MAGL), oltre ad avere un ruolo

chiave nel sistema degli endocannabinoidi, fornisce acidi grassi liberi come molecole segnale a sostegno dello sviluppo tumorale. Abbiamo sviluppato una nuova classe di inibitori di MAGL a base di benzilpiperidina, tra cui è emerso il composto 13 come il più promettente per capacità inibitoria e meccanismo reversibile. Dopo aver osservato l'over-espressione di MAGL nel PDAC e aver dimostrato la sua importanza come fattore di prognosi, abbiamo testato l'effetto del nuovo inibitore. Il composto 13 è in grado di indurre apoptosi e ridurre le capacità migratorie delle cellule PDAC, oltre a presentare un effetto sinergico con la GEM. I risultati ottenuti suggeriscono che questa nuova classe di inibitori di MAGL potrebbe essere sviluppata e dar origine a nuovi agenti farmaceutici per il trattamento del cancro al pancreas.

Nell'ultima parte dello studio abbiamo analizzato i livelli di espressione genica di MAGL in relazione con lo stato mutazionale di p53 al fine di individuare i sottogruppi tumorali più responsivi. Nel PDAC, infatti, sono molto frequenti mutazioni nel gene *TP53* che danno origine a proteine mutate (mutp53) con nuove attività oncogene (mutazioni gain-of-function, GOF) coinvolte nelle alterazioni metaboliche tipiche dei tumori aggressivi e chemioresistenti. Abbiamo osservato che mutanti GOF di p53 aumentano i livelli di mRNA intracellulari di MAGL, mentre wt p53 regola l'espressione genica in senso opposto. Inoltre, il composto 13, l'inibitore di MAGL precedentemente analizzato, risulta più efficace nelle cellule che portano mutazioni GOF di p53. I risultati ottenuti suggeriscono l'uso di inibitori MAGL come potenziale terapia per trattare i pazienti PDAC con gene *TP53* mutante.

In conclusione, la tesi propone due nuovi agenti antitumorali che potrebbero essere usati per il trattamento dei tumori PDAC particolarmente resistenti: molecole di GEM in grado di rilasciare ossido nitrico (NO-GEMs) e inibitori di MAGL a base di benzilpiperidina selettivi e reversibili. Le prime agiscono su meccanismi di resistenza diretti alla GEM aumentandone la concentrazione all'interno delle cellule grazie all'uso dell'NO; i secondi, agiscono a livello del metabolismo lipidico impedendo la formazione di molecole segnale. L'utilizzo degli inibitori di MAGL è stato ulteriormente studiato e viene proposto come target therapy per pazienti

PDAC aventi mutazioni GOF del gene *TP53* particolarmente coinvolte nella progressione tumorale.

## 2. ABSTRACT

According to the prediction of the Global Cancer Observatory (GCO), an interactive web platform that presents global cancer statistics, pancreatic ductal adenocarcinoma (PDAC) will be second cause of death in Western societies within the next decade.

To date, the overall survival of patients at 5 years after diagnosis is only 6%, and 25% in patients undergoing surgical resection, but these represent only 15% of total cases. These data emphasize the need to find new effective drug treatments. Indeed, current therapeutic approaches have great limitations such as chemoresistance, both innate and acquired after the treatment, lack of biomarkers for prediction of therapy response, and intrinsic toxicity of chemotherapeutic agents that causes several side effects.

In this thesis we described three different approaches to overcome chemoresistance in PDAC, which remains a great therapeutic challenge in the field of modern oncology. In the first part, we aimed to counteract several resistance mechanisms directly involved in the metabolism of the drug gemcitabine (GEM). Seven novel gemcitabine pro-drugs capable of releasing nitric oxide (NO-GEMs) within cells were synthesized to enhance the efficacy of GEM by exploiting the anti-tumor effects of NO. Among them, 5b was selected as the most effective. After encapsulation in liposomes to improve its entry into cells, we showed that NO released from 5b causes nitration and inhibition of efflux transporter (MRP5) activity. This results in intracellular accumulation of GEM and increased apoptotic cell death in GEM-resistant PDAC cells, which express MRP5 at higher levels than GEM-sensitive cells. Our results provide a preclinical evaluation of the use of NO-GEM pro-drugs as a novel anticancer strategy to effectively target GEM-resistant PDAC cells.

In the second part of the study, we targeted the metabolic remodeling that cancer cells enact to adapt to the challenges of the microenvironment and facilitate their survival, proliferation, and metastasis formation. Specifically, the enzyme monoacyl glycerol lipase (MAGL), in addition to playing a key role in the endocannabinoid system, delivers free fatty acids as signal molecules to support tumor development. Thus, a new class of benzylpiperidine-based MAGL inhibitors

was developed, among which compound 13 emerged as the most promising for inhibitory capacity and reversible mechanism. After observing MAGL over-expression in PDAC, we tested the effect of the new inhibitor. Compound 13 is able to induce apoptosis and reduce the migratory capacity of PDAC cells, as well as presenting a synergistic effect with GEM. The obtained results suggest that this new class of MAGL inhibitors could be developed and give rise to new pharmaceutical agents for the treatment of pancreatic cancer.

In the last part of the study, we analyzed MAGL gene expression levels in relation to p53 mutational status in order to identify the most responsive tumor subgroups. In PDAC, in fact, mutations in the *TP53* gene giving rise to mutated proteins (mutp53) with new oncogenic activities (gain-of-function mutations, GOF) involved in metabolic alterations typical of aggressive and chemoresistant tumors, are very frequent. We observed that GOF mutants of p53 increase intracellular MAGL mRNA levels, whereas wt p53 regulates gene expression in the opposite direction. Furthermore, compound 13, the previously analyzed MAGL inhibitor, is more effective in cells carrying GOF mutations of p53. The results obtained suggest the use of MAGL inhibitors as a potential therapy to treat PDAC patients with mutant *TP53* gene.

In conclusion, this thesis highlights two novel anticancer agents that could be used for the treatment of particularly resistant PDAC tumors: gemcitabine molecules capable of releasing nitric oxide (NO-GEMs) and selective and reversible benzylpiperidine-based MAGL inhibitors. The first ones act on mechanisms of direct resistance to GEM by increasing its concentration inside the cells through the use of NO; the second ones, act at the level of lipid metabolism by preventing the formation of signal molecules. The use of MAGL inhibitors has been further studied and are proposed to may be use as target therapy to treat PDAC patients with GOF mutant p53 R273H.



### 3. ABBREVIATION LIST

2-AG, 2-arachidonoylglycerol  
ABC transporter, ATP binding cassette transporter  
BIM, Bcl-2-like protein 11  
BLC-2, B-cell lymphoma 2  
BRCA2, breast cancer gene 2  
BSA, bovine serum albumin  
CAF, cancer-associated fibroblast  
DAF-FM, 4-Amino-5-methylamino- 2',7'-difluorofluorescein  
DBD, DNA binding domain  
dCK, deoxycytidine kinase  
DNA, deoxyribonucleic acid  
DNE, dominant negative effect  
eCBs, endocannabinoids  
ECM, extra cellular matrix  
EDTA, ethylenediaminetetraacetic acid  
EMT, epithelial-to-mesenchymal  
FPKM, Fragments Per Kilobase Million  
FPKM, fragments per kilobase million  
GAPDH, Glyceraldehyde-3-Phosphate Dehydrogenase  
GCO, global cancer observatory  
GEM-R, gemcitabine-resistant  
GEM-S, gemcitabine-sensitive  
GEM, gemcitabine  
GFP, green fluorescent protein  
GOF, gain of function  
*h*CNT, human concentrative nucleoside transporter  
*h*ENT, human equilibrative nucleoside transporter  
IPMNs, intraductal papillary mucinous neoplasms  
L-NAME, N( $\gamma$ )-nitro-L-arginine methyl ester  
LD, lipid droplets

LKB1, liver kinase B1  
LOH, loss of heterozygosity  
MAGL, monoacylglycerol  
MCN, mucinous cystic neoplasm  
MDR, multi drug resistant  
MGLL, MAGL gene name  
MLH1, mismatch repair genes MutL Homolog 1  
MLH2, mismatch repair genes MutL Homolog 2  
MLH6, mismatch repair genes MutL Homolog 6  
MMP9, matrix metalloproteinase 9  
mRNA, messenger ribonucleic acid  
MRP, multi drug resistant protein  
Mutp53, mutant protein 53  
NO-GEM, nitric oxide-gemcitabine  
NO, nitric oxide  
ONOO<sup>-</sup>, peroxyxynitrite  
OS, overall survival  
p53, protein 53  
PAAD, pancreatic adenocarcinoma  
PanINs, pancreatic intraepithelial neoplasia  
PBS, phosphate buffered saline  
PDAC, pancreatic ductal adenocarcinoma  
PTIO, 2-Phenyl-4,4,5,5-tetramethylimidazoline-1-oxyl 3-oxide  
RT-PCR, real time – polymerase chain reaction  
SD, standard deviation  
SDS, sodium dodecyl sulphate  
SEM, standard error of the mean  
SiRNA, short interfering ribonucleic acid  
SRB, Sulforhodamine B  
TP53, tumor suppressor 53  
TUNEL, terminal deoxynucleotidyl transferase (TdT) dUTP Nick-End Labeling  
WT, wild type



## 4. TABLE OF CONTENTS

1.	SOMMARIO .....	4
2.	ABSTRACT .....	7
3.	ABBREVIATION LIST.....	9
4.	TABLE OF CONTENTS .....	12
5.	INTRODUCTION.....	16
5.1	The pancreas .....	16
5.2	Pancreatic cancer epidemiology .....	16
5.3	Pancreatic ductal adenocarcinoma pathogenesis features .....	17
5.4	Tumor suppressor p53 .....	18
5.5	Mutant p53 gain-of-function.....	21
5.6	Therapies.....	23
5.7	Gemcitabine .....	24
5.8	Pancreatic cancer chemoresistance .....	25
5.9	Transporters abnormalities .....	26
5.10	Fatty acid metabolism in cancer and its role in chemoresistance .....	27
5.11	Microenvironment reprogramming and tumor crosstalk .....	30
5.12	Gemcitabine resistance mechanisms .....	31
5.13	Nitric oxide (NO) and chemoresistance.....	32
6	MATERIALS AND METHODS .....	35
6.1	Drugs and chemicals.....	35
6.2	Novel NO-GEMs pro-drugs synthesis .....	35
6.3	Novel MAGL reversible inhibitors synthesis .....	36
6.4	Liposome synthesis and purification .....	37
6.5	Cell culture.....	38
6.6	Cell proliferation/ growth inhibition assays.....	38

6.7	DNA damage assay.....	39
6.8	Intracellular analysis of GFP .....	40
6.9	Intracellular drug accumulation assay .....	40
6.10	Cell cycle analysis .....	40
6.11	Apoptosis assay.....	41
6.12	Western blotting.....	42
6.13	Analysis of intracellular NO .....	42
6.14	MRP5 detection, nitration and activity .....	43
6.15	MRP5 silencing.....	44
6.16	Evaluation of MAGL mRNA expression in pancreatic cancer cells .....	44
6.17	Analysis of cell migration.....	44
6.18	Evaluation of pharmacological interaction between MAGL inhibitor and gemcitabine .....	45
6.19	qPCR assays to evaluate key determinants in migration, apoptosis induction and gemcitabine activity .....	45
6.20	Transient transfection and knockdown assay .....	46
6.21	Statistical analysis.....	46
7	AIM OF THE STUDY .....	48
8	RESULTS .....	52
8.1	MRP5 nitration by NO-releasing gemcitabine encapsulated in liposomes confers sensitivity in chemoresistant pancreatic adenocarcinoma cells <sup>91</sup> .....	52
8.1.1	Different GEM cytotoxic effect on GEM-resistant and GEM-sensitive cell lines..	52
8.1.2	The combined treatment of GEM and NO-donor increases the cytotoxic effect in GEM-R cells.....	54
8.1.3	Selection of the most effective NO-GEM pro-drug synthesized.....	55
8.1.4	The delivery of 5b encapsulated in liposomes increases its cytotoxic effects in GEM-R cells.....	56
8.1.5	The intracellular release of NO by 5b or Lipo 5b is determinant to increase their cytotoxic effect.....	60
8.1.6	MRP5 nitration by 5b or Lipo 5b confers chemosensitivity to GEM-R cells .....	62
8.2	New selective and reversible MAGL inhibitor synergizes with GEM and represents a promising anticancer agent for the treatment of pancreatic cancer .....	65
8.2.1	MAGL expression in pancreatic cancer correlates with a poor overall survival.....	65

8.2.2	Novel MAGL inhibitor show higher cytotoxic effect on aggressive PDAC primary culture	66
8.2.3	In more aggressive primary cell model, inhibitor 13 increases apoptosis, and the effect is higher when combined with GEM	67
8.2.4	Inhibitor 13 shows anti-migratory effect in PDAC3	68
8.2.5	Synergistic interaction of compound 13 with GEM and potential mechanisms underlying its effects on apoptosis, migration, and potentiation of GEM activity	70
8.3	Mutant p53 R273H isoform supports MAGL overexpression in PDAC cells	72
8.3.1	MGLL gene expression is higher in patients with mutated forms of TP53	72
8.3.2	Mutants TP53 enhanced MGLL gene expression in PDAC cell lines	73
8.3.3	Chemical inhibition of MGLL gene counteracted mutp53-dependent hyperproliferation	75
8.3.4	Cross-talk between p53 and NF- $\kappa$ B in the regulation of MAGL	78
9	DISCUSSION	80
10	CONCLUSIONS	86
11	BIBLIOGRAPHY	87



## 5. INTRODUCTION

### 5.1 The pancreas

The pancreas is a gastrointestinal organ located in the abdominal cavity. It consists of two structurally distinct but functionally integrated glandular systems: the endocrine and exocrine pancreas. The endocrine pancreas is made up of islets of Langerhans (alpha-, beta-, delta-, PP-, and epsilon- cells) and its role is to modulate blood sugar through the secretion of hormones such as glucagon, insulin, and somatostatin. The exocrine component, occupies more than 80% of the total pancreatic volume and is made up of pancreatic acinar cells and ductal cells. The acinar cells produce and secrete enzymes that have digestive function like  $\alpha$ -amylase, lipase, and protease, which are responsible of nutrients absorption. Pancreatic ductal cells support the activation of the digestive enzymes in the duodenum through the secretion of sodium bicarbonate ( $\text{HCO}_3^-$ ) which provides the optimal pH for the enzymatic digestion.

These physiological functions can be impaired by genetic alterations within the cells that cause the onset of a tumor mass.

### 5.2 Pancreatic cancer epidemiology

Pancreatic cancer is an aggressive and lethal disease with such a poor prognosis that it is expected to become the second leading cause of cancer death in Western societies within a decade.<sup>1</sup> According to the latest report on cancer mortality in Europe, in 2021 were estimated more than 84.000 deaths from pancreatic cancer.<sup>2</sup> In Italy in 2020 it is estimated that 14.300 new diagnoses. Data for 2021 are not available yet, but 12.900 victims are estimated<sup>3</sup>. Among the most common cancers, pancreatic cancer remains the only one not to show a substantial reduction in mortality rates in the last thirty years in Europe. Indeed, only 6% of patients survive five years after the diagnosis.



Diagnosis is prevalent in patients >65 years of age, with a similar incidence rate between the sexes and with expected rates of 8.1 per 100,000 in men and 5.6 in women in EU<sup>2</sup>. The onset of this tumor type is not only related to aging but also to several modifiable, non-modifiable and other heritable risk factors<sup>4</sup>. In particular, despite being considered a moderate risk factor, cigarette smoking plays an important role triggering about 20% of cases<sup>5</sup>. In addition to age, metabolic alterations including obesity, diabetes and chronic pancreatic disease are the predominant non-modifiable risk factors. The factors with the highest risk are those derived from family history, although they represent only 10% of the total cases. Especially mutations in breast cancer gene 2 (BRCA2), which represent the most common inherited mutations in familial pancreatic cancer. Moreover, genetic aberrations of several care-taker genes are associated to cancer syndromes, such as DNA mismatch repair genes MutL Homolog 1 (MLH1), MutS Homolog 2 (MSH2) and 6 (MSH6), or BCRA1 and liver kinase B1/serine/threonine kinase 11 (LKB1) and represent an increased risk<sup>6</sup>.

### 5.3 Pancreatic ductal adenocarcinoma pathogenesis features

More than 90% of pancreatic cancers arise in ductal cells, pancreatic ductal adenocarcinoma (PDAC). PDAC is a multifactorial disease, its onset is the result of sequential genetic alterations and can arise from different precursor lesions (Figure 1). Conventional PDAC mainly originates from pancreatic intraepithelial neoplasia (PanINs 1-3), but few cases arise from cystic lesions as intraductal papillary mucinous neoplasms (IPMNs) and mucinous cystic neoplasm (MCN)<sup>7</sup>. Mucinous tumors are less common and less invasive compared to the ductal subtype.

Although, PDAC is a molecularly heterogeneous disease, mutations in four genes are highly common in the pathogenesis. *KRAS* mutations are the earliest genetic alterations which give rise to the PanIN-1 lesions and are present in 92% of cases. The RAS family of GTPase includes more than 150 small G proteins that regulate several physiological processes such as cell proliferation, differentiation, migration,

and apoptosis. Mutated form of those proteins in the tumor are blocked in their activated form thus promoting tumorigenesis. Anyway, a mutation of *KRAS* is necessary but not sufficient to give rise to PDAC but is required the inactivation of tumor suppressors *CDKN2A*, *TP53*, and *SMAD4* that are the driving force of PDAC development<sup>8</sup>. *CDKN2A* alterations, along with cellular immortalization triggered by telomeric abnormalities, drive tumor progression toward PanIN-2. Mutations of *TP53* and *SMAD4* characterize the most advanced forms of PanIN. The mutational load correlates with the risk of invasiveness of PDAC.

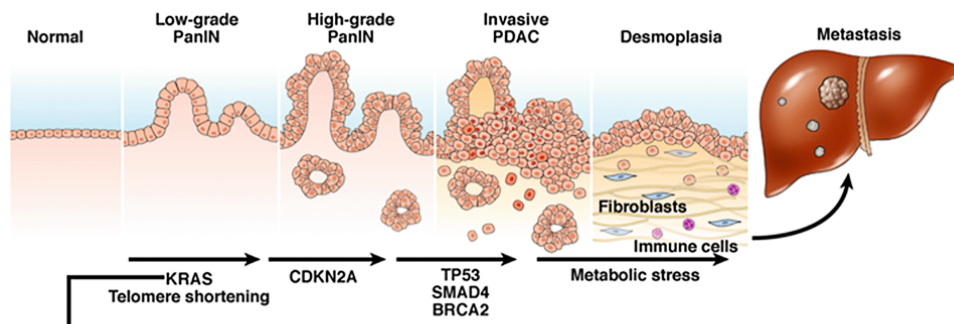


Figure 1. Molecular pathobiology in pancreatic ductal adenocarcinoma.<sup>9</sup>

The major hallmark of pancreatic cancer is the presence of an extensive dense fibrous stroma. This growth of excessive amount of scar tissue around the tumor, which can account for up to 90% of total tumor volume, is clinically defined as desmoplastic reaction<sup>10</sup>. Desmoplasia is characterized by significant overproduction of extracellular matrix (ECM) components, such as collagen and hyaluronic acid and other proteins, and extensive proliferation of activated fibroblasts, myofibroblasts, inflammatory cells, and pancreatic stellate cells (cancer-associated fibroblast, CAF)<sup>11, 12</sup>.

This abundant tissue has an active role in the contribution of tumor growth and dissemination, mainly with the release of cytokines and growth factors. Indeed, there is an active crosstalk between tumor microenvironment and tumor cells.

#### 5.4 Tumor suppressor p53

Physiologically tumor suppressors genes block the transformation of normal cells to cancerous cells counteracting various stimuli of altered cellular homeostasis, such as DNA damage or oncogene activation, by inducing cell cycle arrest, apoptosis or senescence<sup>8</sup>. The loss of these “guardians”, in concert with the mutation of an oncogene driver, pushes the tumor towards its progression.

Among the tumor suppressors, p53 protein, which takes the name from its molecular weight of 53 kDa, is described as “the guardian of the genome” and “cellular gatekeeper” referring to its key role in preserving genomic stability by preventing mutations<sup>13</sup>.

*TP53* is located on the short arm of chromosome 17 and it encodes for p53, a transcriptional factor of 393 amino acids harboring 4 functional domains: acidic transactivation, DNA-binding, oligomerization- and regulatory domain; respectively from the N-terminal to the C-terminal (Figure 2A). In particular, the acidic transactivation domain contains a proline-rich domain essential for the binding to transcription factors and regulators of p53 activity. The DNA-binding domain allows the protein to exert its tumor suppressive function as a transcription factor through regulation of its target genes. The oligomerization domain contains a nuclear export signal involved in the tetramerization of p53 (the active form of this protein). The C-terminal domain has regulatory function including three nuclear localization signals, which are relevant for the post-translational modifications<sup>14</sup>.

In the absence of stress signals, p53 is present at low levels, because its transcription and degradation are finely regulated. Indeed, excessively high levels of p53 can be lethal to cells, whereas too low levels can allow cancer development. The balance is preserved by negative regulators, such as MDM2, COP1 and Pirh2, which are E3 ubiquitin ligases that mediate p53 proteasomal degradation<sup>13</sup>.

In response to various cellular stresses, p53 is stabilized, not only at the transcriptional and translational levels, but mainly by different post-translational modifications, which leads to p53 activation through upstream mediators (i.e. ATM, CHK and ARF) and repression mediated by MDM2<sup>15</sup>. Following its stabilization, p53 tetramers bind directly and specifically DNA responsive elements

(p53 RE) to regulate transcription of target gene, which are estimated more than 3.600.

Depending on the cell and tissue, the type and intensity of stress signals, p53 can block the cell cycle, regulate the DNA repair machinery, promote cell death (apoptosis, ferroptosis or autophagy) of highly damaged cells or senescence, maintain genomic integrity and prevent tumor formation (Figure 2B).

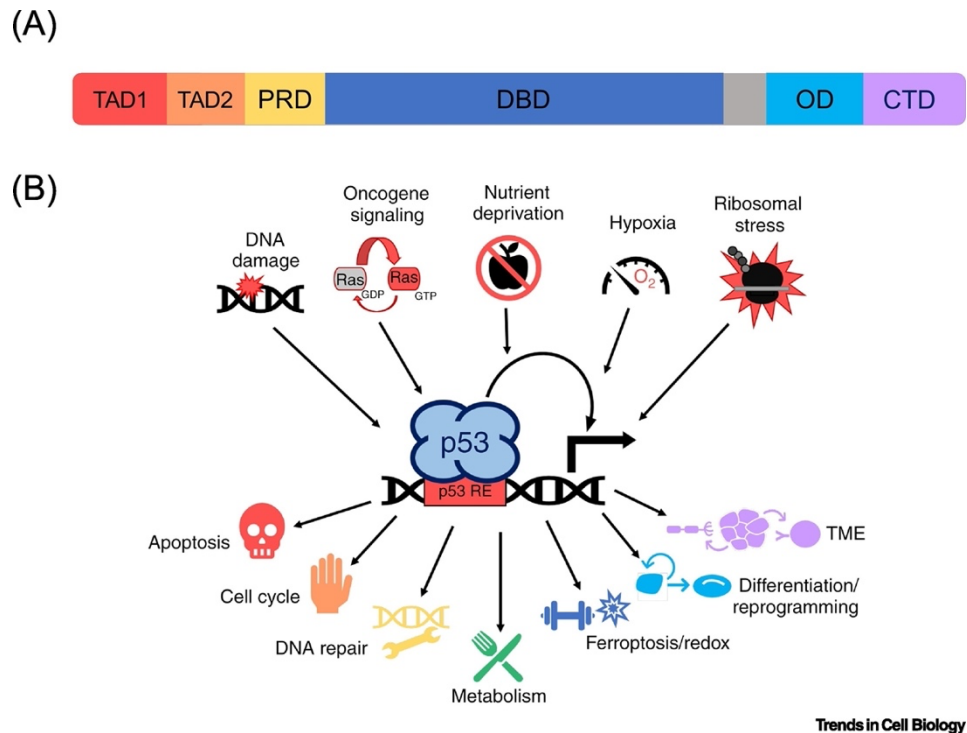


Figure 2. (A) p53 protein domains: transcriptional activation domain (two amino-terminal transcriptional activation domains (TADs) and the proline-rich domain (PRD)), sequence-specific DNA binding domain (DBD); oligomerization domain (OD); and C-terminal domain (CTD). (B) p53 is activated by various cellular stresses, driving a transcriptional response that impacts a wide range of cellular processes.<sup>16</sup>

As shown in Figure 2B, p53 contributes to the modulation of cellular metabolism, including the regulation of glycolysis, pentose phosphate pathway, mitochondrial oxidative phosphorylation and lipid metabolism, whose deregulation is an important hallmark of tumor cells.

## 5.5 Mutant p53 gain-of-function

p53 function is lost in at least 50% of human cancers. Mutations in *TP53* are not essential for the initiation of cancer but facilitates progression of the disease, providing the plasticity required to adapt to the dynamic tumor ecosystem.<sup>17</sup> Thus, inactivation of p53 is definitely an advantage for cancer cells. Cancers with mutant p53 (mutp53) are more aggressive and often resistant to chemo- and radiotherapies.

In PDAC, *TP53* is impaired in 70% of tumor cases as consequence of gene deletion (induced by deletion, insertion or frameshift substitution) or missense mutations.

The majority of p53 mutations are missense mutations, which usually lead to the production of the full-length mutant protein<sup>13</sup>. Most amino acid substitutions occur at the DNA binding domain (DBD), leading to loss DNA-binding capacity and abrogating the transcriptional factor function. There are two types of mutations: the first directly affects the protein's DNA-binding site (contact mutations such as R248Q and R273H); the second, creates local (R249S and G245) or global (R175H and R282W) conformational changes that impair the protein's folding and consequently the ability to bind to DNA<sup>18</sup>. The amino acids R175, G245, R248, R249, R273, and R282 are considered “mutational hot-spot” (Figure 3).

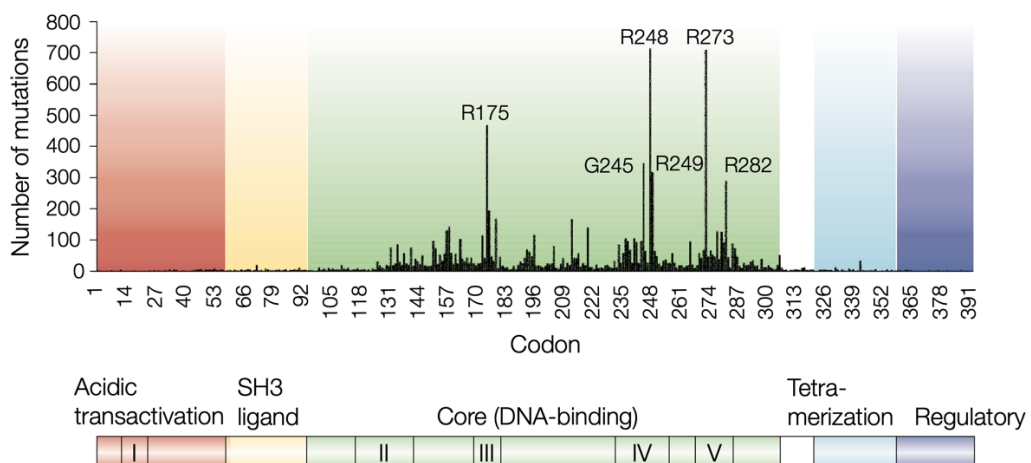


Figure 3. The distribution of hot-spot mutations along the *TP53* sequence.<sup>19</sup>

*TP53* missense mutations can occur in two different ways among cancers: caused by concomitant deletion of the other allele, or due to a mutation in only one allele. The first case, that is the most frequent (60%), is termed as “loss of heterozygosity” (LOH) which results in abrogating the tumor suppressor function of the affected *TP53* allele. The other case is termed “dominant negative effect” (DNE), because p53 mutants play a repressing role on the wild type p53 protein. Indeed, p53 mutants retain the ability to form a protein-tetramer complex (heterodimer complex) which is a mixture of mutated and wild type proteins, where the wild type function is suppressed by its normal DNA-binding activity (Figure 2) <sup>14</sup>.

Intriguingly, missense mutations of p53 not only cause the loss of physiological role in regulating cell fate, but also cause the gain of a number of new oncogenic functions independent of the activities of the wild-type protein. For this reason, they are referred to as gain-of-function (GOF) mutations. GOF p53 supports tumor aggressiveness by several mechanisms, including proliferation, deregulation of cell metabolism, pro-survival signaling, inhibition of apoptosis, drug-resistance, enhanced inflammation, angiogenesis and invasiveness <sup>13, 17,20</sup>.

Thus, in contrast to the wild-type, mutant p53 protein usually accumulates to a high level in tumors.

Losing its normal ability to bind DNA, mutp53 protein directly interacts with some transcription factors or repressors, thus altering the expression of several mRNA and microRNAs a key role in the regulation of tumor progression<sup>21</sup>.

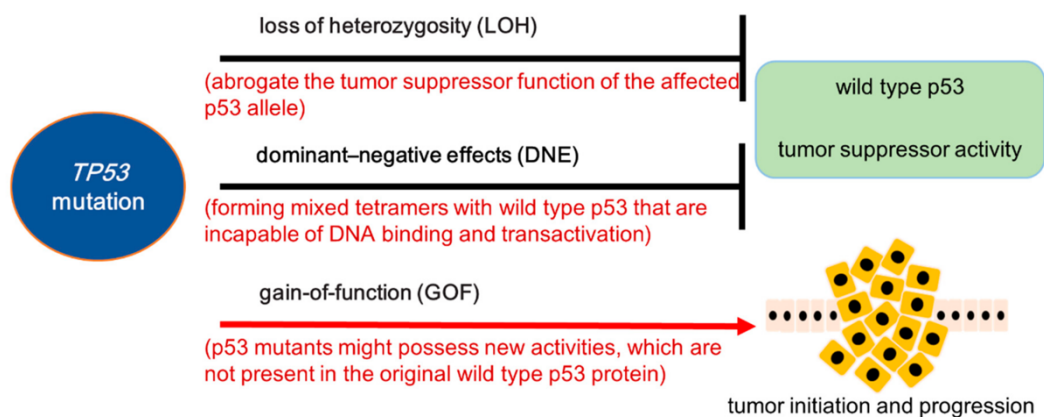


Figure 4. Graphical representation of the consequences of somatic *TP53* mutations in tumorigenesis. The LOH (loss of heterozygosity) and DNE (dominant-negative effect) are

*the two main mechanisms that abrogate the tumor suppressor function of wild type p53. Missense mutations in p53 lead to gain of new function (GOF) that can promote tumorigenesis.*<sup>14</sup>

An increasing knowledge of the genetic alterations within the tumor has highlighted a variability in the molecular pathology. Cancer subtyping is mandatory to better recognize tumor characteristics in term of progression and chemoresistance giving the possibility to treat the individual patient's tumor in the best way possible.

## 5.6 Therapies

PDAC patients are categorized as resectable (R), borderline resectable (BR), locally advanced (LA), and metastatic (MTX). Treatment is diversified depending on the stage of the disease, but the only therapy considered potentially curative is surgical resection with microscopically free margins. To increase the chances of successful surgery, patients may receive preoperative treatment with chemotherapeutics. Unfortunately, resectable tumors account for only 15% of all cases. In fact, it is rare for tumors to be diagnosed in the early stages of development while still localized. However, 5-year overall survival of these patients is still low and limited to 20-25%. Indeed, patients have a high risk of tumor recurrence even after curative-intended resection. Usually, patients after surgery are treated with adjuvant chemotherapy such as gemcitabine, 5-fluorouracil, or other combinations to try to prevent relapse.

Palliative cancer treatments including radiation therapy and chemotherapy are given to patients with advanced disease treatments are diversified based on the performance status (PS) of patients according to Eastern Cooperative Oncology Group (ECOG). Patients with a good PS (0 or 1), are treated with FOLFIRINOX (oxaliplatin, irinotecan, leucovorin, and 5-fluorouracil) or gemcitabine + nab-paclitaxel (GA). While for patients with poor PS, gemcitabine or combinations with 5-fluorouracil are standard treatments<sup>22</sup>. These combinations of treatments are considered the gold standards for PDAC patients.

## 5.7 Gemcitabine

Despite being approved 25 years ago, gemcitabine (alone or in combination) still plays an important role in the treatment of PDAC, both as a preoperative adjuvant treatment and as a treatment of advanced cases<sup>22</sup>.

Gemcitabine (GEM) is a nucleoside analogue of cytidine (2',2'-difluorodeoxycytidine; dFdC), whose biomedical activity is derived from the substitution of the hydrogens of carbon-2' in deoxycytidine with germinal fluorines.

As a pro-drug, after the intracellular uptake, gemcitabine must be phosphorylated by deoxycytidine kinase (dCK) in the active diphosphate (dFdCDP) and triphosphate (dFdCTP) nucleosides, which are the two active metabolites<sup>23</sup>. GEM can be transported into cells by nucleoside active transporters (NTs): sodium dependent (concentrative, hCNT1, hCNT2, hCNT3) or sodium independent (equilibrative, hENT1, hENT2). Although, uptake is primarily mediated by hENT1<sup>24</sup>.

The cytotoxicity of this compound is almost entirely related to the inhibition of DNA metabolism acting against specific enzymes involved in DNA replication and repair processes<sup>25</sup>. The drug acts by blocking the polymerization of DNA after its incorporation into newly synthesized strand. Thanks to a masked chain termination, DNA-repair is prevented killing proliferating cells or leading to a G1 growth arrest that induces apoptosis<sup>26</sup>.

Active GEM, once phosphorylated to dFdCTP, reduces competing free physiological dCTPs for incorporation into DNA, decreasing their available pool and thus potentiating the anti-tumoral effect (Figure 5). This effect is achieved by the inhibition of three enzymes: ribonucleotide reductase (RR), cytidine triphosphate synthetase (CTP synthetase) and deoxycytidylate deaminase (dCMP deaminase)<sup>23</sup>.

Moreover, GEM is able to induce reactive oxygen species (ROS), as a secondary mechanism of action<sup>27</sup>. Indeed, ROS are finely regulated in pancreatic cancer. As demonstrated in our previous studies, in early stages of cancer an increase in ROS correlates with tumor progression but excessive ROS production can cause cellular



damage and promote apoptosis. For this reason, cell lines with lower ROS basal levels are more resistant to GEM<sup>28, 29</sup>.

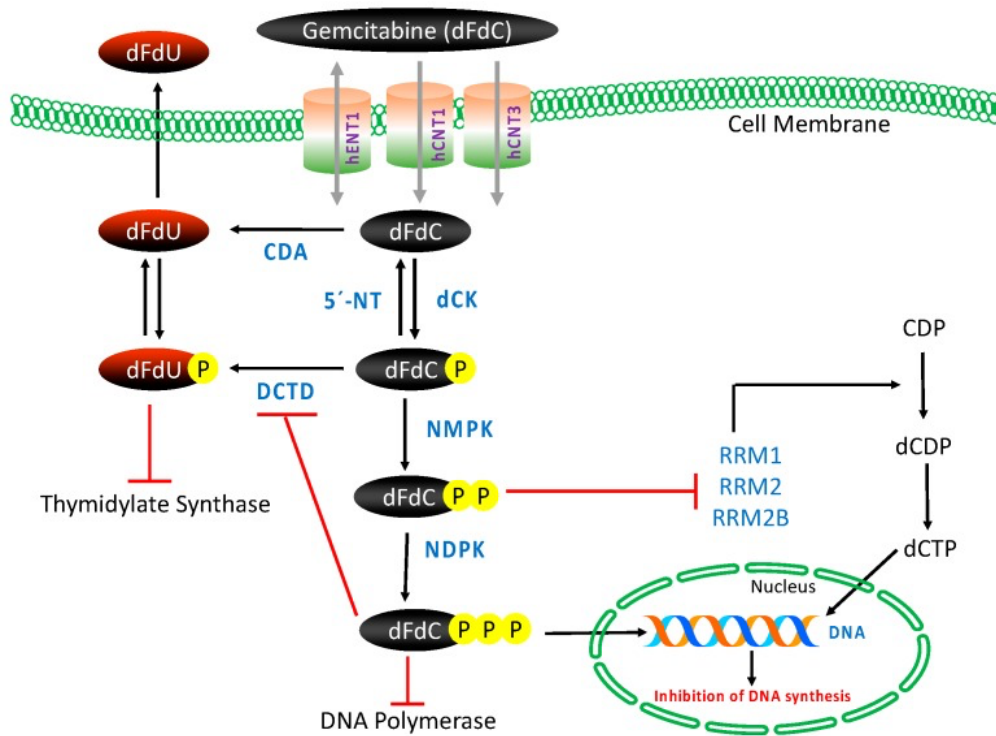


Figure 5. Mechanism of Gemcitabine transport, intracellular activation/deactivation and action. CDA: cytidine deaminase, dCK: deoxycytidine kinase, DCTD: deoxycytidylate deaminase, dFdC: 2',2'-difluorodeoxycytidine, dFdU: 2',2'-difluorodeoxyuridine, hENTs and hCNTs: human nucleoside transporters, NDPK: nucleoside diphosphate kinase, NMPK: nucleoside monophosphate kinase, RR(M1/M2), ribonucleotide reductase, 5'-NT: 5'-nucleotidase.<sup>10</sup>

## 5.8 Pancreatic cancer chemoresistance

The main challenges of PDAC are the early diagnosis and drug resistance. Indeed, most of the diagnoses are made in an advanced, or even metastatic, stage, because patients are often asymptomatic up to that time. Moreover, the lack of biomarkers and screening methods, makes it difficult to detect the tumor in the early stages. However, even for patients with resectable tumors the chance of long-term survival

is low due to relapses. There are three main causes of relapse: poor therapeutic results as adjuvant surgical treatment, undetected micrometastasis, and the development of chemical resistance<sup>24</sup>.

Drug resistance may be “innate” when it occurs from the beginning of the treatment, or “acquired” when it develops during the therapy<sup>30</sup>. Although PDAC cells are susceptible to GEM, most patients develop resistance within a few weeks of treatment. Moreover, prolonged single drug administration may lead to the development of resistance to a variety of agents with different structures, known as cross resistance or multidrug resistance (MDR).

There are multiple factors contributing to the development of chemoresistance in pancreatic cancer, and include transporters abnormalities, metabolic rearrangements, epithelial-to-mesenchymal (EMT) transitions, and changes in tumor microenvironment<sup>24,31,32</sup>. This is the reason why pharmacological treatments fail and resistance still remains a challenge.

### 5.9 Transporters abnormalities

Among the transporters, over the years a great deal of interest has emerged around ATP-binding cassette (ABC) transporter family, one of the major mechanisms related to drug efflux that impairs the therapeutic effect and correlating with patients poor prognosis. These efflux pumps are multidrug resistance proteins (MRPs), in fact they can extrude various types of molecules, such as ions, hormones, sugars, peptides, lipids and xenobiotics. They also play roles in defending against oxidative stress, detoxification and antigen presentation<sup>33</sup>. Therefore, ABC transporters have the ability to influence several pathways and biological processes including carcinogenesis. As evidence of this, high expression levels of ABC transporters have been reported in several types of cancer, compared to normal tissue and correlated with prognosis<sup>34</sup>. The expression profile of this family of transporters seems to be cancer specific. In particular, in PDAC seven MRP genes were found up-regulated: ABCB4, ABCB11, ABCC1, ABCC3, ABCC5, ABCC10, and ABCG2<sup>35</sup>. The mechanism of this regulation is still not

completely clear, although their overexpression is reported to be driven by oncogenes. For example, ABCB1, ABCC1, ABCC5 and ABCG2 modulation is reported to be dependent on p53 status<sup>36</sup>. Among them, the expression level of ABCC5 gene (or multi drug resistant protein 5, MRP5) transporter mRNA levels, although not related to tumor grade or to tumor stage, is regulated during the tumor development<sup>37, 38</sup>. The role of this family of transporters in GEM extrusion is controversial<sup>39, 40</sup>, but its implication in therapeutic resistance is confirmed by several studies<sup>38, 40, 41, 42, 43, 44</sup>. This suggests its involvement in cancer progression via drug resistance mechanisms. MRP expression and ATPase activity increase in a time and dose-dependent manner after treatment with GEM in parental HEK293 syngeneic cells and also in PDAC cell lines with acquired GEM-resistance, suggesting a MRP5 involvement in the decrease drug efficacy<sup>38, 40</sup>. Furthermore, MRP5 overexpression in cells, is associated with an increased resistance to GEM long-treatment<sup>40</sup>.

Interestingly, MDR transporters can be disseminated through microvesicles to normal cells thus spreading the resistant phenotype<sup>45</sup>.

#### 5.10 Fatty acid metabolism in cancer and its role in chemoresistance

Fatty acids (FA) are building blocks of several lipid species, such as phospholipids, sphingolipids and triglycerides, and are composed of a carboxylic acid group and a hydrocarbon chain of varying carbon lengths and degrees of desaturation. They can be also transformed into more complex species, such as diacylglycerides and triacylglycerides, or converted into phosphoglycerides, such as phosphatidylserine<sup>46</sup>.

This large and diverse pool of lipids is involved in various biochemical processes during cancer metabolic reprogramming, which is rightfully part of cancer hallmarks. In this context, fatty acids play a key role being an essential energy source under conditions of metabolic stress, coping to tumor cell proliferation<sup>33</sup>. Tumor cells present an increased *de novo* fatty acid synthesis to produce membrane structural components and to contribute to energy homeostasis,

via storing energy as triacylglycerides in lipid droplets (LDs) <sup>50</sup>. For example, in breast cancer fatty acids synthase (FAS) is highly expressed, and correlated to a poor prognosis<sup>51</sup>. In PDAC the *de novo* synthesis of lipids facilitates GEM resistance.<sup>52</sup> In addition, cholesterol and its downstream metabolites also promote tumor aggressiveness and the development of GEM resistance by increasing the free FA pool and activating the PI3K/Akt pathway<sup>53</sup>.

In this scenario, it is interesting to note that several GOF p53 mutants support lipid accumulation, which could further contribute to cancer progression through the upregulation of enzymes involved in mevalonate pathway, or the inhibition of AMPK<sup>54</sup>.

Lipids support membrane biosynthesis and remodeling to adapt to different environmental conditions and ensure proliferation and survival.<sup>55</sup> Cancer cell membranes have unique lipidic compositions that differ from those of normal cells. The composition also allows to predict the degree of aggressiveness of the tumor, because membrane architecture has an impact in migration and metastasis dissemination<sup>56</sup>.

A metabolomic profiling of PDAC revealed that glycerophospholipids are the most altered metabolites between resistant and sensitive tumors treated with different drugs, including gemcitabine<sup>55</sup>.

Surprisingly, classes of ABC transporters (ABCA and ABCG) play a role in membrane remodeling by increasing their fluidity via extrusion of cholesterol from the membrane. Other transporters, including ABCC5<sup>57</sup>, are floppases able to change the asymmetric composition of the cell membrane exposing elevated levels of phosphatidylserine (PS) decreasing the permeability, and therefore drugs delivery<sup>58</sup>.

Moreover, fatty acids generate lipids messengers that activate pro-tumor pathways. An important class of bioactive lipids are the eicosanoids, molecules with pro-inflammatory and pro-tumorigenic effects, such as prostaglandins (in particular PGE2, which is involved in a signaling axis that promote self-renewal<sup>59</sup>), thromboxanes and leukotrienes. Eicosanoids are synthesized from arachidonic acid (AA).

In the last decade, a growing interest has emerged around the enzyme monoacylglycerol lipase (MAGL) as this enzyme is involved in cancer progression through different mechanisms. MAGL is a serine hydrolase (33kDa), firstly discovered having a role in lipolysis where it catalyzes the hydrolysis of monoacylglycerols into glycerol and free fatty acids (FFAs). Except for the *de novo* synthesis, this is the main process to generate fatty acids. FFAs can generate secondary lipid metabolites, including lysophospholipids especially lysophosphatidic acid (LPA), known for their oncogenic role<sup>60, 61</sup>. LPA is a potent oncogenic lipid modulator that support tumor progression activating pathways of survival, proliferation, migration and EMT, such as phospholipase C, PI3K-AKT, RAS-ERK, RHO and RAC GTPases and NF- $\kappa$ B<sup>60, 59</sup>.

Interestingly, MAGL impairs FFA levels specifically in aggressive tumors, but not in normal tissues where it primarily controls MAGs levels.<sup>62</sup> MAGL high expression was found to be correlated to worse prognosis in hepatocellular carcinoma, prostate and colorectal cancers<sup>59</sup>.

MAGL also breaks down the endocannabinoid monoacylglycerol 2-arachidonoylglycerol (2-AG), in arachidonic acid (AA). 2-AG is a bioactive lipid, which is not only an eicosanoids precursor, but also an agonist of cannabinoid receptors (CB1 and CB2). CB1 and CB2 mRNA and protein were found to be expressed in PDAC cell lines and in several biopsies, but basically undetectable in normal pancreatic tissue.<sup>63</sup> Endocannabinoids, as well as exogenous cannabinoid drugs, are considered very promising anti-cancer treatments, due to their capacity to inhibit tumor progression or activate cell death mechanisms of apoptosis or autophagy<sup>48, 63, 64</sup>. Moreover, they are able to inhibit cancer migration and EMT pathways<sup>48, 65</sup>. For these reasons, endocannabinoids system became a target for cancer treatment.

Given the ability of MAGL to provide FFA to compensate for glucose deprivation periods, generate lipids precursors for membranes synthesis and oncogenic lipid signaling mediators,<sup>48</sup> together its prognostic value in several types of tumors, it has attracted great attention as potential therapeutic target in recent years.

### 5.11 Microenvironment reprogramming and tumor crosstalk

Cancer cells metabolic reprogramming most commonly arises from the tumor microenvironment (TME). Indeed, metabolic reprogramming is not exclusive to cancer cells, but also involves cells of the TME that are remodeled to support tumor growth, progression and evasion from therapies.<sup>47</sup> TME and its crosstalk with tumor cells, are crucial aspects in the low response rate to chemotherapies. TME represents a physical and biochemical barrier to chemotherapy contribute to hypoperfusion and hypoxia, reducing chemotherapeutic drugs activity.

As previously mentioned, desmoplastic reaction is a fundamental feature of PDAC and it is composed by 20% of cancerous cells and 80% of stroma components (stellate cells, cancer-associated fibroblasts, endothelial, and immune cells), extra-cellular matrix (ECM), and blood and lymphatic vessels. In particular, the major components are pancreatic stellate cells (PSCs) and cancer-associated fibroblasts (CAFs), which derive from PSCs.

CAFs has a constitutive activated phenotype obtained by epigenetic regulation, which actively support tumorigenesis in different ways. Activated CAFs promote tumor progression and migration through autocrine and paracrine cell-to-cell communication secreting cytokines and interleukins.<sup>33</sup> In addition, CAFs can translocate metabolic substrates trough exosomes. As reported from Zhao et al. exosomes can contain lactate, acetate, amino acids, lipids, and tricarboxylic acid (TCA) cycle intermediates that promote metabolic switch of cancer cells, known as Warburg effect, from mitochondrial OXPHOS to anaerobic glycolysis via miRNA and substrates transfer.<sup>66, 67</sup>

An interesting feature of PDAC is the failure of cancer treatments based on immunotherapies, although these types of treatments have recently revolutionized oncology<sup>67</sup>. Indeed PSCs, activated by hypoxia, regulate T-cells migration preventing them from infiltrating in the tumor. This is the reason why PDAC is considered a “cold tumor” with low T-cells infiltration and low tumor mutation burden with few neoantigens, which makes immunotherapy difficult to apply successfully<sup>68</sup>.

Interestingly, in breast cancer, ABC transporters were found also related to TME remodeling, overexpressed by some component cells, they are able to send paracrine signals by transferring resistance to chemo-sensitive neighboring cells and an elusive immune response by reprogramming macrophage activity<sup>69</sup>.

The failure of immunotherapy is the reasons why chemotherapy in PDAC remains the first line therapeutic regimen and drug resistance mechanisms remain an issue of fundamental importance.

### 5.12 Gemcitabine resistance mechanisms

While efforts have been made to find new drugs, understanding mechanisms of chemoresistance remains mandatory.

Despite the approval of clinical new combination treatments such as FOLFIRINOX, or its new fluorouracil-free modification, GEM-based treatments are a cornerstone in all stages of PDAC. However, its clinical efficacy is seriously compromised by tumor-related molecular mechanisms of cellular resistance.

Several mechanisms of resistance directed to GEM have been described: some are linked to its uptake, activation and metabolism, and others are specific to the tumor and its microenvironment, which, plays critical roles in the development of chemoresistance.

GEM passes the plasma membrane entering the cells thanks to the nucleoside transporters hENTs and hCNTs. Of relevance is the hENT1 transporter, that has high affinity for GEM and mediates the majority of GEM uptake in vivo. GEM pharmacological response is influenced by hENT1 levels<sup>24</sup>. High expression of the transporter correlates with a better overall survival and disease-free survival<sup>70</sup>. Conversely, loss of hENT1 leads to the onset of resistance, highlighting its value as a prognostic indicator for those patients for whom adjuvant therapy would be indicated<sup>71, 72, 73, 74</sup>.

Furthermore, a recent study demonstrated that hENT1 expression level correlates with alterations in glucose metabolism during the development of Warburg effect-related chemoresistance<sup>75</sup>. In cells that have become resistant to GEM after

prolonged treatment, the transporter regulates glucose flux and glycolysis in a clinically relevant manner. hENT1 may reverse chemoresistance by down-regulating glycolysis<sup>76</sup>.

Once in the cells, the limiting step in the activity of GEM concerns its activation into active metabolites. The main enzyme that phosphorylates the molecule is deoxycytidine kinase (dCK). This enzyme is often inactivated in PDAC and when overexpressed chemosensitivity is restored; so, it represents one of the major drivers of resistance to GEM and probably the best prognostic biomarker.<sup>77</sup>

Other enzymes are implicated in GEM resistance by acting on its intracellular metabolism as cytidine deaminase, 5'-nucleotidase, and ribonucleotide reductase. Cytidine deaminase (CDA) acts by inactivating dFdC to dFdU. dFdU cannot be phosphorylated by pyrimidine nucleoside phosphorylases and it is therefore degraded. This is a clinically relevant resistance mechanism, indeed, in GEM + nab-paclitaxel (GA) treatment, nab-paclitaxel synergizes with GEM by reducing CDA protein levels via ROS induction<sup>78</sup>.

5'-nucleotidase competes with dCK through the dephosphorilation of dFdCMP. High levels of 5'-nucleotidase in epithelial murine cells correlate with lower concentrations of active metabolites<sup>79</sup>.

Ribonucleotide reductase (RR) converts ribonucleotides to dNTPs, the DNA building blocks. The formulation of GEM as a pro-drug allows its potentiation, because dFdCDP induces the inhibition of RR consequently decreasing the available physiological dNTPs. Decrease in intracellular GEM levels, caused by other resistance mechanisms, triggers feedback of synthesis of new dNTPs by activating RR. Moreover, from cells exposed to long treatment emerge clones with high levels of RR expression developing strong resistance to GEM<sup>80</sup>.

### 5.13 Nitric oxide (NO) and chemoresistance

Nitric oxide (NO) is a gas and a free radical known to have very important physiological roles. It is considered a relatively stable free radical and under certain



biological conditions reacts with only two types of molecules: metals and other free radicals<sup>82</sup>.

Biologically, NO is mainly synthesized in endothelial cells from L-arginine by the family enzymes NO-synthases (NOS). Nitric oxide biosynthesis consists of a series of reactions that convert L-arginine and O<sub>2</sub> into NO and L-citrulline, depending on the availability of certain cofactors such as NADPH, FAD, and BH<sub>4</sub>. There are three forms of NOS: neuronal (nNOS), inducible (iNOS) and endothelial (eNOS). Despite the name, they are expressed by multiple tissues and different types of cells. Among these enzymes, relevant differences exist in the mechanism of activation and in the levels of NO production.<sup>83</sup> nNOS and eNOS are activated by a Ca<sup>+</sup>-dependent mechanism: they catalyze NO following an increase in intracellular Ca<sup>+</sup> amount. As the name implies, iNOS is instead inducible by mediators of inflammation, which increase the transcriptional activation of the gene encoding for the enzyme, increasing its expression and NO synthesis. The nNOS produces NO in nanomolar amounts, while the eNOS produces NO within micromolar concentrations in a transient manner thus generating vasodilation. Instead, iNOS is constantly activated and not regulated by Ca<sup>+</sup> concentrations. iNOS expressed by macrophages and other inflamed cells produces NO in millimolar concentrations.<sup>84</sup> The interesting thing is that different intracellular levels of NO have different effects. Nano to micro-molar concentrations (produced by eNOS and nNOS) have physiological effects in cellular respiration or vasodilation/angiogenesis. In contrast, persistent high millimolar concentrations can lead to cell death, while low levels produced during inflammation promote mutagenesis<sup>85</sup>.

NO plays a role in several pathological conditions, such as cardiovascular, pulmonary, neurodegenerative, infectious, and cancerous diseases. In tumor biology, its effect is controversial in the literature because it shows stimulatory or inhibitory effects on cancer progression and metastasis. This dual effect is concentration- and dose-dependent. Low levels of NO induce tumor progression and improvement in tumor perfusion, but high levels reduce it and sensitize the tumor to chemo- and radiotherapy<sup>86</sup>.

Indeed, low levels of NO can modify the tumor microenvironment, mainly by promoting angiogenesis and regulating the immune system, promoting the Warburg

effect and tumor resistance. On the other hand, high levels of NO are prone to generate DNA mutations under chronic conditions of inflammation that are normally controlled by cell through pathway of DNA-damage repair or apoptosis. These mutations or damages become critical in the presence of mutated p53 leading to carcinogenesis. Moreover, high NO can activate immune system to counteract the tumor<sup>85</sup>.

NO is a highly lipophilic and diffusible molecule, so it can reach a target at some distance from where it is synthesized. NO can promote the S- nitrosylation<sup>87</sup> of redox-sensitive cysteines or can react rapidly with other radicals, such as singlet oxygen generating the strong oxidant peroxynitrite (ONOO-)<sup>88</sup>. ONOO- induce the tyrosine nitration of proteins changing their conformation and activity. Nitration is involved in multiple biological processes, including signal transduction, protein degradation, energy metabolism, mitochondrial dysfunction, enzyme inactivation, immunogenic response, apoptosis, and cell death<sup>89</sup>. A strong link emerged between NO and the mechanism of resistance to cancer chemotherapy. Indeed, it has been demonstrated that it can revert resistance to doxorubicin in colon cancer cells by inhibiting efflux drug-related pumps through direct tyrosine nitration<sup>90</sup>.

## 6 MATERIALS AND METHODS

### 6.1 Drugs and chemicals

Gemcitabine (2',2'-difluoro-2'-deoxycytidine; GEM) was provided by Accord Healthcare (Milan, Italy) and solubilized in dimethylsulfoxide (DMSO) (Invitrogen, Thermo Fisher) to a final concentration of 10 mM; the solution has been aliquoted and stored at -20°C.

Gemcitabine, used in Amsterdam at Giovannetti's lab, was a generous gift from Eli-Lilly (Indianapolis, IN) and was dissolved in sterile water.

NO-donor (Diethylamine NONOate diethylammonium salt  $\geq 98\%$ ) was provided by Sigma-Aldrich (Milan, Italy), stored at -80°C. It was freshly solubilized in phosphate buffered saline (PBS) (Gibco, Thermo Fisher) for each experiment.

NO-GEMs pro-drugs as well as MAGL inhibitors were solubilized in DMSO and diluted in culture medium before use. All other chemicals were purchased from Sigma-Aldrich (Zwijndrecht, The Netherlands).

### 6.2 Novel NO-GEMs pro-drugs synthesis

The NO-releasing gemcitabine conjugates (NO-GEMs) are new synthesis compounds by our collaborators at the University of Turin.<sup>91</sup> They are chemically obtained by adding appropriate NO moieties at 4-position of drug through an amide bond (Figure 6). The hydrolysable amide linkage is present in the orally available N4-valproyl gemcitabine (LY2334737), N4-squalenoyl gemcitabine (SQdFdC) and in N4-steroyl gemcitabine (C18dFdC) three modified GEMs with improved bioavailability properties. The nitric moieties are organic nitrates (nitric esters) that release NO through enzymatic pathway. These are attached to the drug in different number among the new pro-drugs. The designed models have been synthesized through standard methods of the organic chemistry. All the products have been

characterized by classical physical methods (IR, NMR, Mass Spectrometry, elemental analysis). The purity has been checked by RP-HPLC method.

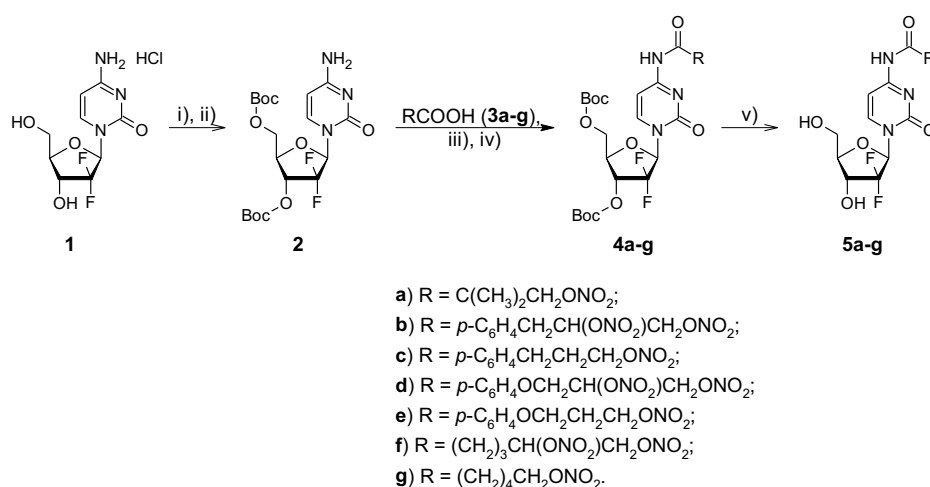


Figure 6. Novel synthesized NO-GEMs prodrugs.

### 6.3 Novel MAGL reversible inhibitors synthesis

Compound 13 is a new *in vitro* reversible MAGL inhibitor designed and synthesized by collaborators at the University of Pisa. Compounds were designed by searching for all the chemical moieties potentially able to fit in the MAGL active site by examining the structures of many serine hydrolase inhibitors reported in literature. After studies with docking software, they created several new compounds using the most active existing ones as initial scaffolds, among which a fatty acid amide hydrolase (FAAH) inhibitor. Compound 13 is the final compound, a benzylpiperidine derivative, which simultaneously possesses the best chemical portions of the previous compounds: a trifluoromethyl group in position 4 of the pyridine ring and a 2-fluoro-5-hydroxyphenyl amide portion.

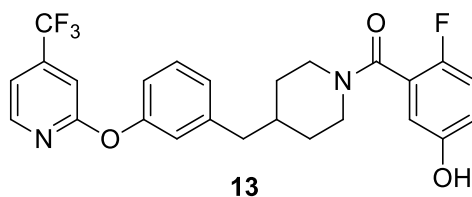


Figure 7. Structure of compound 13.

Compounds were tested for their inhibitory activity *in vitro* on human MAGL by adopting a spectrophotometric method.<sup>92</sup> Moreover, all the compounds were also evaluated for their inhibitory activity on human FAAH, to determine their selectivity, since they all derive from a structural optimization of a fragment belonging to a FAAH inhibitor. The enzymatic method used for FAAH assays was similar to that used for MAGL, differing in the used substrate.<sup>93</sup> 13 showed an IC<sub>50</sub> value of 2.0 nM, therefore it represents the most active MAGL inhibitor of this class, still endowed of a high degree of selectivity over FAAH (IC<sub>50</sub> > 10 μM). Compound 13 reversibility was also tested, investigating the effect of dilution on the inhibition activity. The potency was significantly reduced after dilution, as is expected for reversible inhibitors.

#### 6.4 Liposome synthesis and purification

Liposomal 5b (Lipo 5b) is obtained incorporating the compound 5b in liposomes.<sup>91</sup> Liposomes containing the selected 5b NO-releasing prodrug were synthesized as follow.

The liposomes were prepared using the thin layer hydration and extrusion technique<sup>94</sup> starting from a lipid film formed by 5% of polyethylene glycol with saturated C18 stearyl fatty acid (octadecanoic acid) and DSPE: 1,2-Distearoyl-sn-glycero-3-phosphoethanolamine (mPEG-DSPE) and 30% cholesterol (CHOL). This layer was formed adding 6.5 μmol of DSPC (distearoylphosphatidylcholine) in 300 μl of CHCl<sub>3</sub>, 3.0 μmol of CHOL in 300 μl of CHCl<sub>3</sub>, 0.5 μmol of mPEG-DSPE in 300 μl and 1.9 μmol of 5b in 100 μl of methanol and 200 μl of CHCl<sub>3</sub>. This process was assessed in order to maintain a total ratio of DSPC, CHOL, mPEG-DSPE at 6.5:3.0:0.5 and a molar 5b molar ratio of 19% to the total lipid layer. All these molecules were mixed in a single tube and the resulting solution was left in evaporation with low pressure, for about 20 minutes, in rotation in order to produce a lipidic thin layer homogeneous on the container's surface. The unwanted residual traces were eliminated with a vacuum pump for about 1 hour.

This produced thin layer was hydrated with 900  $\mu$ l of HEPES (pH 7.4) buffer at 60 °C under stirring to obtain a homogeneous suspension. Finally, the liposomes were extruded under nitrogen pressure on the polycarbonate filters using by an extruder at 60 °C. All this process was composed by 2 cycles. The first one with filter pore dimension of 0.4  $\mu$ m and the second one with 0.22  $\mu$ m. Both under a low pressure at 5 bar. The synthesized nanoparticles were purified via filtration gel technique with a Sepharose CL-4B contained column. As the elution buffer was used the HEPES.

## 6.5 Cell culture

Cell lines are from pancreatic adenocarcinoma ductal tissue. PANC-1 and MIA PaCa-2 cell lines were grown in DMEM medium (Gibco, Thermo Fisher), supplemented with 10% FBS and 50  $\mu$ g/mL gentamicin sulfate (BioWhittaker, Lonza). AsPC-1 were cultured in RPMI-1640 medium, supplemented with 10% FBS and 50  $\mu$ g/mL gentamicin sulfate (BioWhittaker, Lonza). SUIT-2 cell line (JCRB1094, Tokyo, Japan), and the primary cell cultures PDAC2 and PDAC3 were cultured in RPMI-1640 medium (Lonza, Basel, Switzerland) supplemented with 10% newborn calf serum, penicillin (50 IU/ml), and streptomycin (50  $\mu$ g/ml) from Gibco (Gaithersburg, MD). In addition, the ductal immortalized non-tumor cells hTERT-HPNE cells obtained from ATCC (Manassas, VA, USA) were cultured in DMEM medium with 5% FBS and 10 ng/mL human recombinant EGF. All the cells were incubated at 37 °C, 5% CO<sub>2</sub> and were frequently tested for mycoplasma contamination with the MycoAlert Mycoplasma Detection Kit (Westburg, Leusden, The Netherlands).

## 6.6 Cell proliferation/ growth inhibition assays

Cell proliferation was evaluated by Crystal violet assay as follow. Cells were seeded in 96-well plates ( $5 \times 10^3$  cells/well), 24 h later treated with various

compounds and further incubated for the indicated times (see legends to figures). At the end of the treatments, cells were stained and fixed with a crystal violet solution containing formaldehyde (for a solution of 100 mL: 750 mg of violet crystal powder, 250 mg of NaCl, 4.7 mL of 37% formaldehyde, 50 mL of ethanol and 45.3 mL of bidistilled water) (Sigma, Milan, Italy). The dye was solubilized in phosphate buffered saline (PBS) containing 1% SDS and measured photometrically at 595 nm absorbance by a microplate reader (GENios Pro, Tecan, Milan, Italy) to determine cell growth.

The inhibitory effects on cell growth were evaluated by Sulforhodamine B (SRB) assay. Cells were seeded in 96 well plates at the density of 5000 per well. After 24 hours, once the cell monolayer was formed, cells were treated for 72 hours with MAGL inhibitors (0.1–50  $\mu$ M) or gemcitabine (1–1250 nM). Cells were then incubated for 72 hours, fixed with trichloroacetic acid at 4 °C, washed with deionized water and then dried at RT. After the fixation, the plate was stained with SRB, washed with acetic acid solution, and left to dry again. SRB was resuspended in a Tris base solution and its absorption, was measured at 490 and 540 nm, as described previously.<sup>95</sup> Finally, the half-maximal response concentration ( $IC_{50}$ ) was calculated with GraphPad Prism version 9 (GraphPad PRISM, Intuitive Software for Science, San Diego, CA).

## 6.7 DNA damage assay

The genotoxic damages were evaluated by the Single Cell Gel Electrophoresis assay (Comet assay), as reported previously<sup>96</sup>. Images were quantified by the CometScore software (TriTek Corp., Sumerduck, VA). The DNA dependent proapoptotic damage was measured using the TUNEL Assay Kit - BrdU-Red (Abcam, Cambridge, MA), as per manufacturer's instruction. The image quantification was performed using the ImageJ software (<https://imagej.nih.gov/ij/>), counting 10 microscopic fields, with a minimum of 20 cells/field.

## 6.8 Intracellular analysis of GFP

Cells were seeded in 96-well plates ( $5 \times 10^3$  cells/well) and, the day after, treated with 10  $\mu$ L or 100  $\mu$ L of GFP encapsulated in liposome for 48 h. Cells were washed with PBS to remove liposomes which not entered in cells. GFP fluorescence (em. 485 nm and ex. 535 nm) was measured in HANKS solution by multimode plate reader (GENios Pro, Tecan, Milan, Italy). Values were normalized on cell proliferation by the crystal violet assay.

## 6.9 Intracellular drug accumulation assay

PANC-1 cellular samples derived from compound incubation were diluted 3:1 with acetonitrile 0.1% HCOOH; the mixture was sonicated, centrifuged for 10 min at 2150g, filtered (0.45  $\mu$ m PTFE) and analyzed by RP-HPLC. The concentration of compound was normalized to the protein content and expressed as nmol compound/mg cell proteins.

HPLC analyses were performed with a HP 1200 chromatograph system (Agilent Technologies, Palo Alto, CA, USA) previously described. The samples were eluted on an Aquasil C18 column (200  $\times$  4.6 mm, 5  $\mu$ m, Thermo). The column effluent was monitored by MWD at 270 nm referenced against an 800 nm wavelength. Quantification of compound 5b was done using calibration curve obtained using standard solutions of compound (linearity determined in a concentration range of 0.1–100  $\mu$ M;  $r_2 > 0.99$ ).

## 6.10 Cell cycle analysis

Cells were washed twice with fresh PBS, incubated in 0.5 mL ice-cold 70% v/v ethanol for 15 min, then centrifuged at 1200  $\times$ g for 5 min at 4  $^{\circ}$ C and rinsed with 0.3 mL citrate buffer (50 mM Na<sub>2</sub>HPO<sub>4</sub>, 25 mM sodium citrate, and 0.01% v/v Triton X-100) containing 10 mg/mL propidium iodide and 1 mg/mL RNase (from bovine pancreas). After 15 min incubation in the dark, the intracellular fluorescence



was detected by an EasyCyte flow cytometer (Becton Dickinson, Bedford, MA). For each analysis,  $1 \times 10^4$  events were collected and analyzed by the Incyte software (Becton Dickinson).

### 6.11 Apoptosis assay

Cells were seeded in 96-well plates ( $5 \times 10^3$  cells/well) and, the day after, treated with drugs at the indicated concentrations for 48 h. At the end of the treatments, cells were fixed with 4% paraformaldehyde in PBS at room temperature for 30 min, then washed twice with PBS and stained with annexinV/FITC (Bender Med-System, Milan, Italy) in binding buffer (10 mM HEPES/NaOH pH 7.4, 140 mM NaCl, and 2.5 mM  $\text{CaCl}_2$ ) for 10 min at room temperature in the dark. Finally, cells were washed with binding buffer solution and fluorescence was measured by using a multimode plate reader with excitation and emission filters at 485 nm and 535 nm respectively (GENios Pro, Tecan, Milan, Italy). The values were normalized on cell proliferation by crystal violet assay.

The other apoptosis assay is based on the assessment whether Caspase-3, an enzyme involved in the effector phase of apoptosis, is a downstream target of MAGL inhibitors, its enzymatic activity was measured by a specific spectrofluorimetric activity assay (Human Active Caspase-3 Immunoassay Quantikine® ELISA, Catalog Number KM300, R&D Systems, Inc., Minneapolis, MN). Briefly, cells were plated in 6-well plates ( $5 \times 10^5$  cells/ml) and exposed to the drugs for 24 h at 5X  $\text{IC}_{50}$  or for 72 hours at their  $\text{IC}_{50}$ . At the end of drug incubation cell extracts were diluted and mixed to the reagents according to the manufacturers' protocol. Absorbance was measured at 450 nm, subtracting readings at 540 nm. Relative caspase activity was calculated using a standard curve with human recombinant Caspase-3.

## 6.12 Western blotting

Cells were treated, harvested and washed in PBS, and re-suspended in RIPA buffer (50 mM Tris-HCl pH 7.5, 150 mM NaCl, 1% Igepal CA-630, 0.5% Na-Doc, 0.1% SDS, 1 mM Na<sub>3</sub>VO<sub>4</sub>, 1 mM NaF, 2.5 mM EDTA, 1 mM PMSF, and 1×protease inhibitor cocktail). After incubation on ice for 30 min, the lysate was centrifuged at 14,000g for 10 min at 4 °C and the supernatant collected for the analysis. Protein concentration was quantified by Bradford reagent (Pierce, Milan, Italy) using bovine serum albumin as a standard. Protein extracts (30 µg/lane) were loaded in a 12% SDS-polyacrylamide gel to be resolved and so electro-blotted onto PVDF membranes (Millipore, Milan, Italy). Membranes were incubated with blocking solution (5% low-fat milk in TBST 100 mM Tris pH 7.5, 0.9% NaCl, 0.1% Tween 20) for 1 h at room temperature and probed overnight at 4 °C with a primary Bim (C34C5) Rabbit mAb (Cell Signaling Technology) or GAPDH (14C10) Rabbit mAb (Cell Signaling Technology). Immunodetection was carried out using chemiluminescent substrates (Amersham Pharmacia Biotech, Milan, Italy) and recorded using a Hyperfilm ECL (Amersham Pharmacia Biotech).

## 6.13 Analysis of intracellular NO

Diaminofluorescein-FM diacetate (DAF-FM) probe (Sigma) was used to quantify intracellular NO. Cells were plated in 96-well plates (5 × 10<sup>3</sup> cells/well). 24 h later, the medium was changed with DMEM w/o serum and phenol red and cells were incubated with N $\omega$ -Nitro-L-arginine methyl ester hydrochloride (L-NAME) (Sigma) for 15 min at 37 °C (as describe in figure legend), then, 10 µM DAF-FM for 30 min at 37 °C. Cells were washed with PBS to remove the probe which not entered in cells. Finally, cells were treated with pro-drugs and PTIO (Sigma). After 12 h, DAF-FM fluorescence was measured ( $\lambda_{exc}$  485 nm and  $\lambda_{em}$  535 nm) by a multimode plate reader (GENios Pro, Tecan, Milan, Italy). Values were normalized on cell proliferation by the crystal violet assay.

#### 6.14 MRP5 detection, nitration and activity

For the detection of MRP5 total amount, cells were rinsed with lysis buffer (50 mM Tris-HCl, 1 mM EDTA, 1 mM EGTA, 150 mM NaCl, 1% v/v Triton-X100; pH 7.4), supplemented with the protease inhibitor cocktail III (Cabochem, La Jolla, CA), sonicated and clarified at 13000 ×g, for 10 min at 4 °C. Protein extracts (20 µg) were subjected to SDS-PAGE and probed with an anti-MRP5/ABCC5 antibody (Abcam, Cambridge) or with an anti-actin antibody (Sigma Chemicals. Co.).

For the measurement of nitration and activity of MRP5, membrane-enriched fraction was prepared by ultracentrifugation as described.<sup>97</sup> To detect nitrated or nitrosylated MRP5, 100 µg of proteins from membrane fraction were immunoprecipitated overnight with anti-nitrotyrosine antibody (Millipore, Burlington, MA) or an anti-nitroso-cysteine antibody (Abcam), using 25 µL Pure Proteome Beads A/G (Millipore), then subjected to immunoblotting and probed with the anti-MRP5 antibody. The membranes were probed with the horseradish peroxidase-conjugated secondary antibodies (Bio-Rad), washed with Tris-buffered saline (TBS)/Tween 0.01% v/v. Proteins were detected by enhanced chemiluminescence (Bio-Rad Laboratories). Blot images were acquired with a ChemiDoc™ Touch Imaging System device (Bio-Rad Laboratories).

MRP5 activity was measured by incubating 100 µg of immune-precipitated MRP5 for 30 min at 37 °C with 50 µL of the reaction mix (25 mM Tris/HCl, 3 mM ATP, 50 mM KCl, 2.5 mM MgSO<sub>4</sub>, 3 mM dithiothreitol, 0.5 mM EGTA, 2 mM ouabain, 3 mM NaN<sub>3</sub>; pH 7.0). The reaction was stopped by adding 0.2 mL ice-cold stopping buffer (0.2% w/v ammonium molybdate, 1.3% v/v H<sub>2</sub>SO<sub>4</sub>, 0.9% w/v SDS, 2.3% w/v trichloroacetic acid, 1% w/v ascorbic acid). After a 30 min incubation at room temperature, the absorbance of the phosphate hydrolyzed from ATP was measured at 620 nm, using a Synergy HT Multi-Mode Microplate Reader (Bio-Tek Instruments, Winooski, VT). The absorbance was converted into µmol hydrolyzed phosphate/min/mg proteins, according to the titration curve previously prepared with serial dilutions (100 µM-0.1 nM) of NaHPO<sub>4</sub>.

### 6.15 MRP5 silencing

$1 \times 10^5$  cells were treated with 10 nM of three unique 27mer-siRNA duplexes, targeting MRP5 (#SR306772; Origene, Rockville, MD) or with a Trilencer-27 Universal scrambled negative control siRNA duplex (#SR30004; Origene), as per manufacturer's instructions. The efficiency of silencing was verified by immunoblotting.

### 6.16 Evaluation of MAGL mRNA expression in pancreatic cancer cells

RNA-sequencing analyses for PDAC2 and PDAC3 were performed, as described by Firuzi et al.<sup>98</sup> Raw data were pre-processed for quality filtering and adapter trimming using FASTX Toolkit (version 0.7) and subsequently mapped to the Human genome (GRCh38) using STAR alignment tool (version 2.5.3a). We obtained ~90% of reads mapped to the Human Genome per sample. Gene counts in Fragments Per Kilobase of transcript per Million mapped reads (FPKM) normalization were computed using CuffLinks algorithm and plots were generated with R version 3.5.0. SUIT-2 mRNA expression data was obtained from the Cancer Cell Line Encyclopedia (<https://portals.broadinstitute.org/ccle>).

### 6.17 Analysis of cell migration

Pancreatic cancer cells were seeded in a 96 well plate at the density of 25000 cells/well to form a confluent monolayer after 24 hours. Subsequently, the monolayer was wounded by 96-well pin tool scratcher. Detached cells were washed away with phosphate-buffered saline (PBS). Medium only or medium containing a concentration of 5 times ( $5\times$ ) the  $IC_{50}$  of each drug was added to the wells. Brightfield images were taken with the software Universal Grab 6.3 digital on a Leica DMI300B microscope (Leica Microsystems, Eindhoven, The Netherlands) at

different time points, to be analyzed with Scratch Assay 6.2 software (Digital Cell imaging Labs, Keerbergen, Belgium) as described previously.<sup>95</sup>

#### 6.18 Evaluation of pharmacological interaction between MAGL inhibitor and gemcitabine

The pharmacological interaction between compound 13 and gemcitabine was evaluated by the median drug effect analysis method, as described previously.<sup>99</sup> Compound 13 was added at the inhibitory concentration of 50%, while gemcitabine was added in a drug range between 0 and 1250 nM. The combination index (CI) was calculated to compare cell growth inhibition of the combination and each drug alone. Data analysis was carried out using CalcuSyn software (Biosoft, Oxford, UK). A CI of below 0.8 indicates a synergetic cytotoxic effect. A CI between 0.8 and 1.2 indicates additive effect and above 1.2 indicates antagonistic effect of the combination therapy.

#### 6.19 qPCR assays to evaluate key determinants in migration, apoptosis induction and gemcitabine activity

Real-Time Quantitative Reverse Transcription PCR (qRT-PCR) was performed to evaluate the gene expression of MMP9, BCL-2, BCL-x, and *hENT1*, using  $\beta$ -actin, and GAPDH as housekeeping genes. The cells were seeded at  $3\text{-}5 \times 10^3$  in a 6-well flat bottom plate with 2 ml medium per well and incubated with drugs at  $5 \times \text{IC}_{50}$  for 24 hours. Total RNA was extracted using TRIzol Reagent (15596-026, ThermoFisher Scientific, Waltham, MA) according to the manufacturer's protocol. One  $\mu\text{g}$  of RNA was reverse transcribed using first-strand cDNA synthesis (First Strand cDNA Synthesis Kit; ThermoFisher #K1612) on Bio-Rad machine C100 Thermal Cycler. Real-time qPCR quantification was performed using specific TaqMan detection probes and primers (TaqMan Universal PCR Master Mix #4304437; Thermo Fisher Scientific, USA) with the ABI PRISM-7500 instrument

(Applied Biosystems, Foster City, CA), as described previously.<sup>95</sup> Data obtained were analyzed according to the  $2^{-\Delta\Delta C_t}$  method.

#### 6.20 Transient transfection and knockdown assay

AsPC-1 cells were seeded in 96-well or in six-well plates. Wild type or mutant p53 ectopic expression in p53-null cancer cells was obtained by transfecting pcDNA3-mutp53R273H, or pCMV-wild type p53 expression vectors or their relative negative control (pcDNA3 or pCMV).

Knockdown of p53 expression was obtained by transfecting cells with specific TP53 small interfering siRNA or with a siRNA-CTR (negative control) purchased from Life Technologies.

Transfections were carried out using Lipofectamine 3000 (Thermo Fisher Scientific, Milan, Italy) for 48 h, according to the manufacturer's instructions.

#### 6.21 Statistical analysis

All experiments were performed in triplicate and repeated at least twice. The experimental data were expressed as mean values  $\pm$  standard deviation (SD) or standard error of the mean (SEM). Data were subjected to computerized statistical analysis using T-student test or ANOVA performed by GraphPad Prism 9 software were used to calculate the experimental significance. The level of significance was  $p < 0.05$ .



## 7 AIM OF THE STUDY

The incidence of pancreatic ductal adenocarcinoma (PDAC) is steadily increasing and the survival is the lowest among cancers. It is estimated to become the second leading cause of cancer-related deaths by 2030. Because of the aggressive nature and its resistance to different kinds of therapies, PDAC remains one of the most difficult-to-treat cancers. Therefore, the development of drug resistance is a key factor to understand the failure of current therapy. As chemoresistance is multifactorial, the increase in survival of patients with PDAC should occur at different levels: as for instance, by improving existing therapies, developing new therapeutic strategies, and stratifying patients based on novel biomarkers that can predict response to therapy. Thus, the main goal of this thesis was to investigate tumor chemoresistance by proposing potential new strategies to overcome PDAC chemoresistance.

More specifically, the aims of this thesis can be summarized as follows:

- Improve the historical gold standard drug, GEM, by trying to overcome several of the challenges related to its resistance. We aimed to do this by enhancing GEM cytotoxic effect exploiting NO anti-tumor properties and by improving drug cellular uptake with liposome delivery. Indeed, the antitumor effects of NO-releasing compounds were recently reported further strengthening the concept of hybrid NO-donors as a design strategy.<sup>83</sup> Based on the existing data, the use of nitric oxide alone as a drug development strategy appears weak, but NO can be used in conjunction with other clinical agents to overcome drug resistance and sensitize cancers to cytotoxic agents.<sup>90</sup> To exploit NO as anti-tumor agent, seven new formulations of nitric oxide-releasing gemcitabine (NO-GEMs) were designed, synthesized and then encapsulated in liposomes by our collaborators from University of Turin. The nitric moieties are organic nitrates that release NO through enzymatic pathway and are added to GEM through an appropriate linker that prevent GEM metabolic inactivation in cells.

This strategy could affect efficiently also GEM-resistant PDAC cell triggering the formation of highly cytotoxic ion peroxynitrite in mitochondria of cancer cells through the mitochondrial release of NO and the GEM-mediated production of



mitochondrial superoxide ions ( $O_2^-$ ). This mechanism could also induce the nitration of mitochondrial MDR transporters that might increase the intracellular accumulation of GEM and increase apoptosis and cancer cell death.

Overall, the main aim of this part was to identify novel NO-GEM prodrugs able to overcome PDAC cell resistance to the standard drug GEM. To do this, NO-GEMs have been tested in two different PDAC cell models: PANC-1 and MIA PaCa-2, known to be GEM-resistant and GEM-sensitive PDAC cell lines, respectively. Moreover, after examining the effectiveness of the new compounds, we investigated the possible mechanisms of action of these novel pro-drugs in PDAC cells.

- Overcome chemoresistance by exploiting new anticancer agents that target enzymes involved in the metabolic switch towards tumor progression. Metabolic reprogramming has been shown to play a crucial role in the response of cancer cells to widely-used first-line chemotherapeutics.<sup>100</sup> Lipid metabolism is highly active in tumors due to the high proliferation rate of tumor cells, and therefore their higher need of nutrients and membrane-lipids compared to normal cells. More specifically we focused on monoacylglycerol lipase (MAGL), a new emerging and promising therapeutic target involved in lipid metabolic reprogramming. Indeed, MAGL modulates an oncogenic signaling network to generate pro-tumorigenic lipids which favor cancer invasiveness, migration, and growth.

Therefore, the strategy was to inhibit this enzyme to circumvent resistance by blocking energy delivery and to prevent its pro-tumorigenic signaling. Thus, a new class of potent and highly specific reversible MAGL inhibitors was synthesized by our collaborators at the University of Pisa. These inhibitors were designed by after a careful docking study of ligand-protein interactions. We tested their cytotoxic effect in primary cell culture (PDAC2 and PDAC3) which retain the same features of the original tumor and compared to immortalized PDAC cell model (SUIT-2). Moreover, we investigated MAGL inhibitors potential role in counteracting chemoresistance analyzing the effect of combined treatment with GEM in PDAC3 cells, derived from the most aggressive tumor.

- Stratify patients based on molecular features involved in chemoresistance in order to identify the most effective personalized therapy for the individual tumor. Mutations in the *TP53* gene occur in over 70% of PDAC patients. Most of these alterations are missense mutations resulting in the expression of mutant GOF forms of p53, which contribute to the induction and maintenance of cancer. Since MAGL expression is a very important patients' prognostic factor, we focused more deeply on its possible regulation by hypothesizing that GOF mutant p53 may directly or indirectly regulate MAGL. Indeed, the detailed mechanisms of its up-regulation in cancer remain unknown. WT p53 regulates lipid metabolism<sup>100</sup>, it is therefore conceivable that mutp53 plays a role in the remodeling of lipid metabolism. Thus, through an exploration of public sequencing data, we investigate a potential correlation between MAGL gene expression and p53 mutations. Then, we verified the correlation in different cell models: in a p53-null PDAC cell line (AsPC-1) after the overexpression of mutp53 and in two PDAC cell lines bearing different muted p53 isoforms (PANC-1 and MIA PaCa-2) after the knockdown of p53. Data suggested a role for mutp53 in the overexpression of MAGL in PDAC contributing to a poor clinical outcome. Finally, our data support the usage of MAGL inhibitors as potential therapy to treat PDAC patients harboring mutant *TP53* gene.



## 8 RESULTS

### 8.1 MRP5 nitration by NO-releasing gemcitabine encapsulated in liposomes confers sensitivity in chemoresistant pancreatic adenocarcinoma cells<sup>91</sup>

#### 8.1.1 Different GEM cytotoxic effect on GEM-resistant and GEM-sensitive cell lines

A heterogeneous response to GEM treatment in PDAC has been extensively described, suggesting that different mechanisms of resistance may be associated with different tumor subtypes. We compared the effect of GEM treatment in two PDAC cell lines, PANC-1 and MIA PaCa-2. As shown in Fig. 1, 48 h of GEM treatment determined ~20% cell growth inhibition and ~15% of damaged DNA in PANC-1 cells (Figure 8A), while it caused ~50% cell growth inhibition and ~35% of damaged DNA in MIA PaCa-2 cells (Figure 8B). Representative images of the comet assay performed in the two PDAC cell lines treated with GEM are reported in Fig. 8C. These data support the usage of PANC-1 cells as a model of gemcitabine-resistant (GEM-R) PDAC cells, as compared to gemcitabine-sensitive (GEM-S) MIA PaCa-2 PDAC cells.

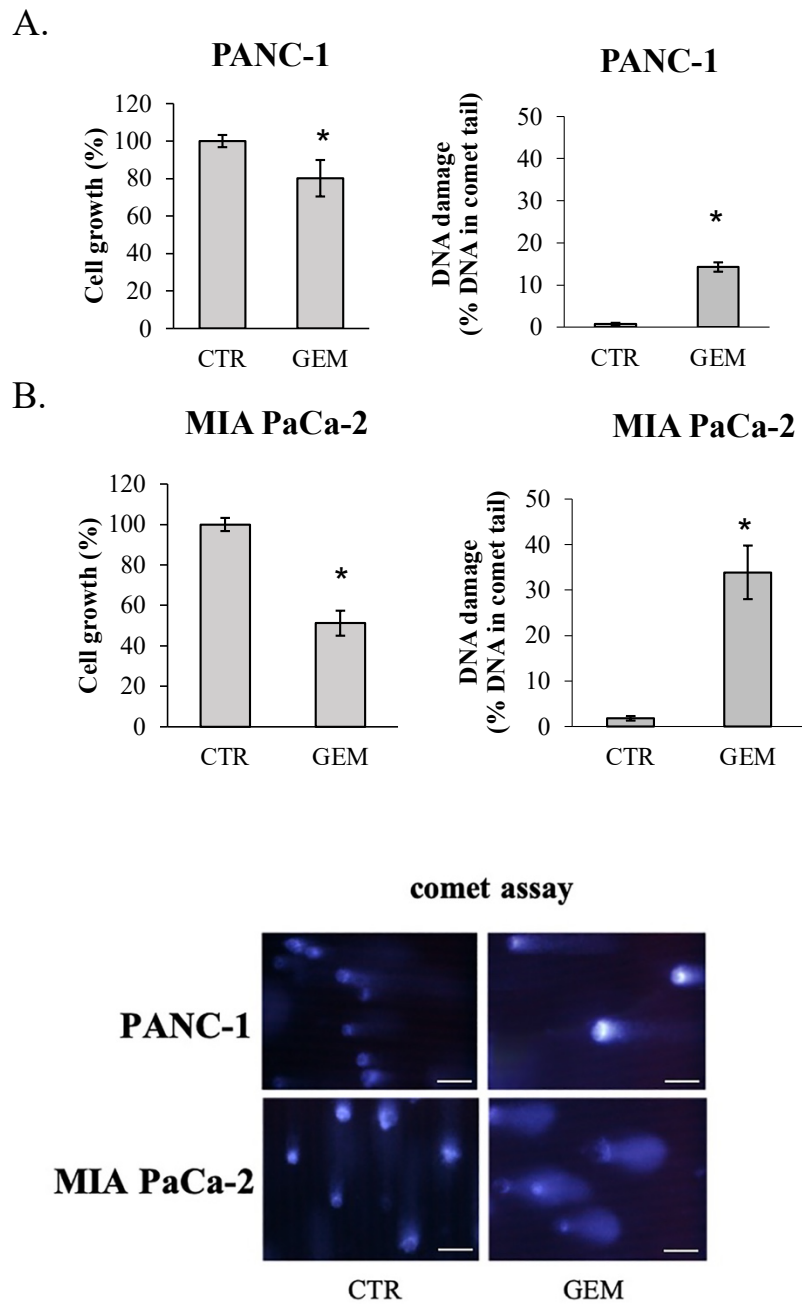


Figure 8. Cytotoxicity of GEM in PANC-1 and MIA PaCa-2 PDAC cell lines. PANC-1 (A) and MIA PaCa-2 (B) cells were treated with 100  $\mu$ M GEM for 48h. C) Representative images of the comet assay in PANC-1 and MIA PaCa-2 cells treated with 100  $\mu$ M GEM for 48h. Measurements were performed in triplicate and data are presented as means  $\pm$  SD ( $n = 3$ ). Student's *t*-test: \* $p < 0.05$  GEM versus CTR.

### 8.1.2 The combined treatment of GEM and NO-donor increases the cytotoxic effect in GEM-R cells

To investigate whether the addition of NO-donors to GEM treatment could increase the cytotoxic effects on PDAC cells we performed cell growth assay on both PANC-1 and MIA PaCa-2 cell lines using increasing concentrations of GEM in association to a non-toxic concentration of the NO-donor diethylamine NONOate. NO-donors are products that can release NO under physiological conditions and that can consequently be used as NO-prodrugs. Given their action as chemo- and radio-sensitizing agents, their long half-lives and specific targeting, we hypothesized that they could enhance the anticancer effect of the standard drug.<sup>101</sup> Thus, we performed cell growth assay on both our cell line models, PANC-1 and MIA PaCa-2, using increasing concentrations of GEM in association to a non-toxic concentration of the NO-donor diethylamine NONOate. As shown in Figure 9, the combined treatment GEM + NO-donor decreased PANC-1 cell growth as compared to GEM treatment alone (panel A), while the same combined treatment didn't enhance cytotoxicity of GEM in MIA PaCa-2 cells (panel B). These data suggest that the intracellular release of NO may enhance the effect of GEM in chemoresistant PDAC cells, thus providing rationale for further investigations with novel synthetic NO-GEM pro-drugs.

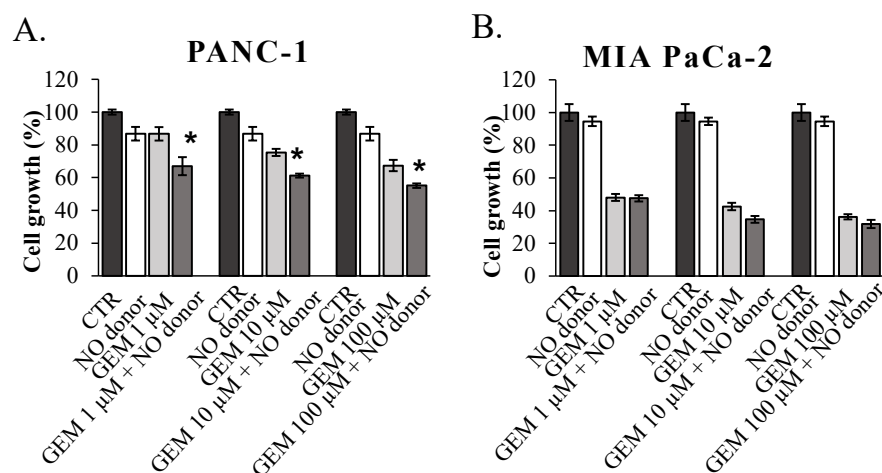


Figure 9. GEM + NO donor combined treatment inhibits GEM-R PANC-1 cell growth as compared to single treatments. PANC-1 (A) and MIA PaCa-2 (B) cells were treated with

*increasing concentrations of GEM and/or 100  $\mu$ M of NO-donor. Measurements were performed in triplicate and data are presented as means  $\pm$  SD ( $n = 3$ ). Student's  $t$ -test:  $*p < 0.05$  GEM + NO donor versus GEM.*

### 8.1.3 Selection of the most effective NO-GEM pro-drug synthesized

Fruttero's team from University of Turin, synthesized 7 novel NO-GEM pro-drugs as described in the "Material and methods" section.

We tested the effects of each NO-GEM pro-drugs in our cell line models and compared them to the GEM-based standard treatment performing a cell growth assay. Although the new pro-drugs have a similar effect, after 48h of treatment, we selected 5b as the most active NO-GEM pro-drug in GEM-R PANC-1 cells (Figure 10A). No improvement was observed in GEM-S MIA PaCa-2 cells as compared to GEM treatment alone (Figure 10B). In support of this data, we investigated the enhanced antiproliferative effect of 5b in chemoresistant cells performing a long-term cell proliferation assay. Cells received a single pulse treatment for 24h with GEM or 5b and, after drug removal, cell growth was analyzed at different time points until 120 h from the beginning of the treatment. The results, shown in Fig. 10C and D, confirm that the pro-drug 5b was significantly more cytotoxic compared to GEM in chemoresistant PANC-1 cells, while its effect in GEM-S MIA PaCa-2 cells was equal to that determined by GEM treatment.

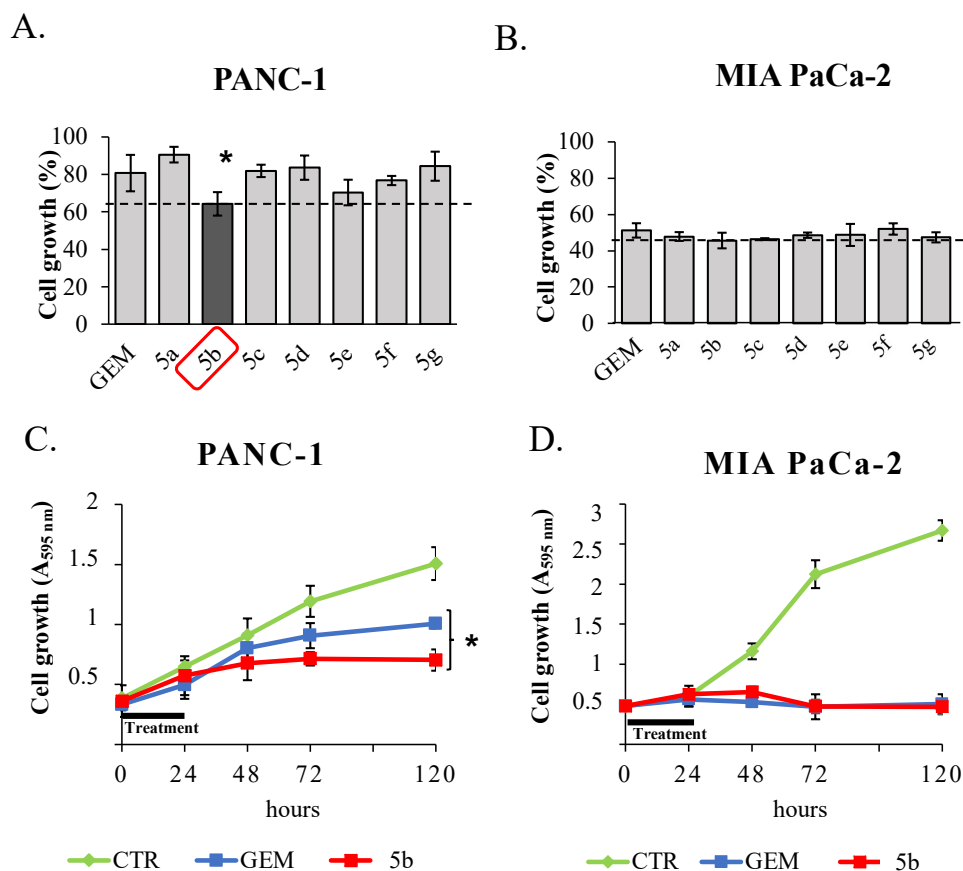


Figure 10. The compound 5b inhibits PANC-1 cell growth more than GEM. Comparison of the cytotoxic effect of GEM and of the seven new-synthesized NO-GEM pro- drugs in PANC-1 (A) and MIA PaCa-2 (B) cells treated with 100  $\mu$ M of pro-drugs for 48 h. cytotoxicity of 10  $\mu$ M GEM or 5b after a 24 h pulse treatment in PANC-1 (C) and MIA PaCa-2 (D) cells. Measurements were performed in triplicate and data are presented as means  $\pm$  SD ( $n = 3$ ). Student's *t*-test: \* $p < 0.05$  5b versus GEM.

#### 8.1.4 The delivery of 5b encapsulated in liposomes increases its cytotoxic effects in GEM-R cells

To facilitate the intracellular uptake of the new pro-drug and to minimize side effects, we asked to Arpicco's lab from University of Turin to insert 5b into liposomes. Liposomes are small unilamellar vesicles with a dimension about 170 nm and they were prepared as described in the "Material and methods" section.



First of all, we tested the transport ability of liposomes after having marked them with the green fluorescent protein (GFP) and we measured its emission intensity inside the cells after 48h. The increasing concentration of GFP into the cells suggests that liposomes are a valuable method for drug delivery in our experimental system (Fig. 11A). We performed a drug-stability assay in order to measure the concentration of GEM effectively released into PANC-1 cells treated with different concentrations of 5b or encapsulated 5b (Lipo 5b) for a short period (4 h) or a long period (24 h). A higher accumulation of GEM into the cells after the treatment with Lipo 5b was detected compared to non-encapsulated drug treatment at each experimental condition tested (Figure 11B).

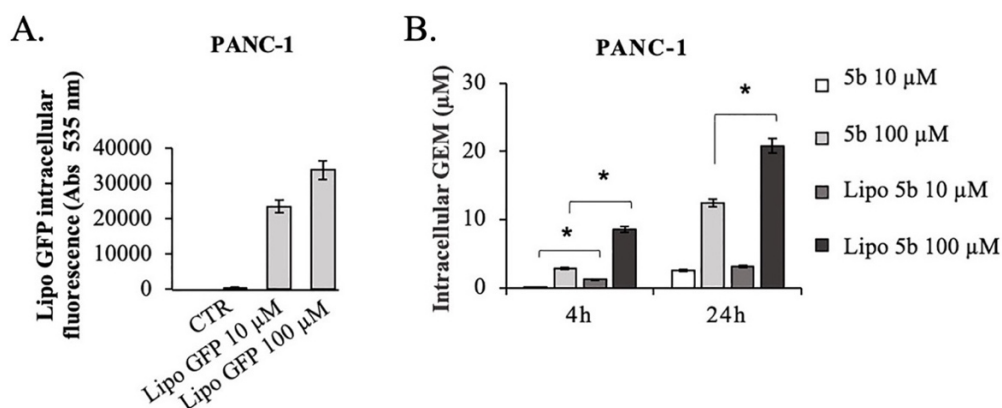
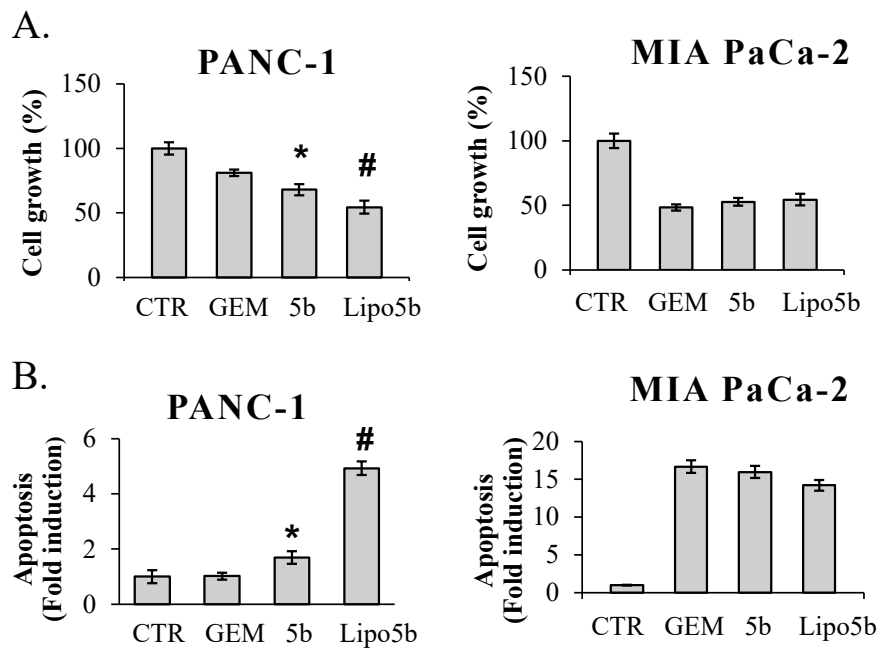


Figure 11. A) Intracellular amount of GFP-released by liposomes after PANC-1 cell treatment with Lipo GFP for 48h. B) Intracellular amount of 5b compound after cell treatment with 10 or 100  $\mu$ M of 5b or Lipo 5b for 4h or 24h in PANC-1 cells. Measurements were performed in triplicate and data are presented as means  $\pm$  SD ( $n = 3$ ). Student's *t*-test: \* $p < 0.05$  Lipo 5b versus 5b.

After testing the validity of the transport system and appreciating the increase in intracellular drug concentration post-treatment, the effect of Lipo 5b was evaluated in comparison to the standard GEM and the 5b pro-drug to prove that its higher intracellular delivery may result in higher cytotoxic effects. As control, we tested the effects of empty liposomes on cell growth without observing any significant alterations (data not shown). As shown in Fig. 12, Lipo 5b determined a higher

inhibition of cell growth (panel A) due to increased stimulation of apoptosis (panel B) in PANC-1 cells, compared to GEM or 5b treatments alone. On the other side, also in encapsulated formulation 5b failed to improve the cytotoxic in MIA PaCa-2 cells. These results suggest that liposome delivery is a useful approach for a further enhancement of pro-drug 5b effect in GEM-R PDAC cells. Accordingly, TUNEL assay confirmed that 5b encapsulation in liposomes strongly enhanced apoptosis in PANC-1 cells, without any improvements in MIA PaCa-2 cells (Fig. 12C). Moreover, we demonstrated that the apoptotic response of PANC-1 cells to GEM, 5b or Lipo 5b is strictly associated to the concomitant stimulation of the pro-apoptotic protein Bim, at both mRNA and protein levels (Fig. 12D), suggesting the triggering of the intrinsic apoptotic pathway after GEM-R cell treatment with Lipo 5b.



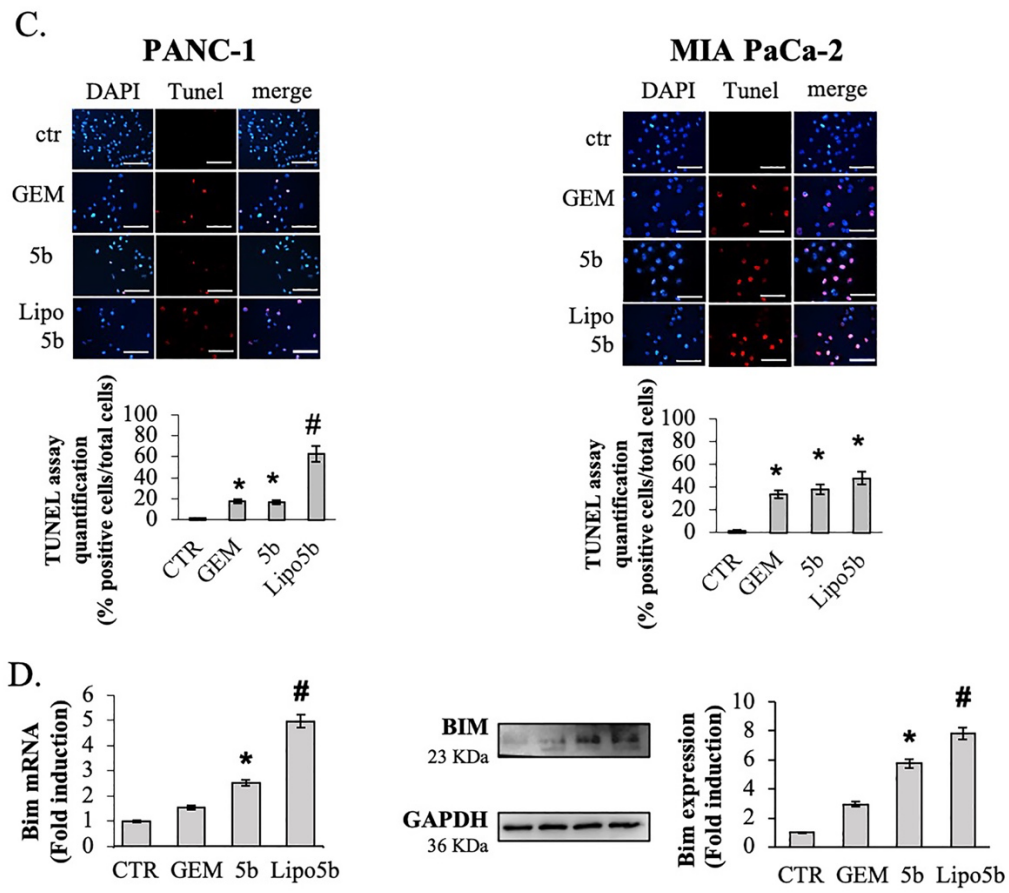


Figure 12. Encapsulation of the compound 5b in liposomes (Lipo 5b) enhances 5b-induced apoptotic cell death in PANC-1 cells. Cytotoxic effect (A) and apoptosis (B) in PANC-1 cells treated with 100  $\mu$ M GEM, 5b or Lipo 5b for 48h. Measurements were performed in triplicate and data are presented as means  $\pm$  SD ( $n = 3$ ). Student's *t*-test: \* $p < 0.05$  5b versus GEM; #  $p < 0.05$  Lipo 5b versus 5b. C) Representative images of three similar experiments and quantification of TUNEL staining in PANC-1 and MIA PaCa-2 cells treated with 100  $\mu$ M GEM, 5b or Lipo 5b for 48h. Student's *t*-test: \* $p < 0.05$  GEM or 5b or Lipo 5b versus CTR; # $p < 0.05$  Lipo 5b versus 5b. D) qPCR and Western blot analysis of Bim expression in PANC-1 treated with 100  $\mu$ M GEM, 5b or Lipo 5b for 48h. Student's *t*-test: \* $p < 0.05$  5b versus GEM; # $p < 0.05$  Lipo 5b versus 5b.

Concerning a possible involvement of the cytostatic effect on cell growth inhibition induced by the drugs, we analyzed the percentage of cells in the various phases of the cell cycle after treatments. Figure 6 shows that GEM, 5b and Lipo 5b didn't

significantly affect cell cycle distribution in PANC-1 cells, while treatments increased the percentage of the GEM-S MIA PaCa-2 cells in the pre-G0 hypodiploid phase, a phenomenon associated with the induction of apoptosis in these cells.

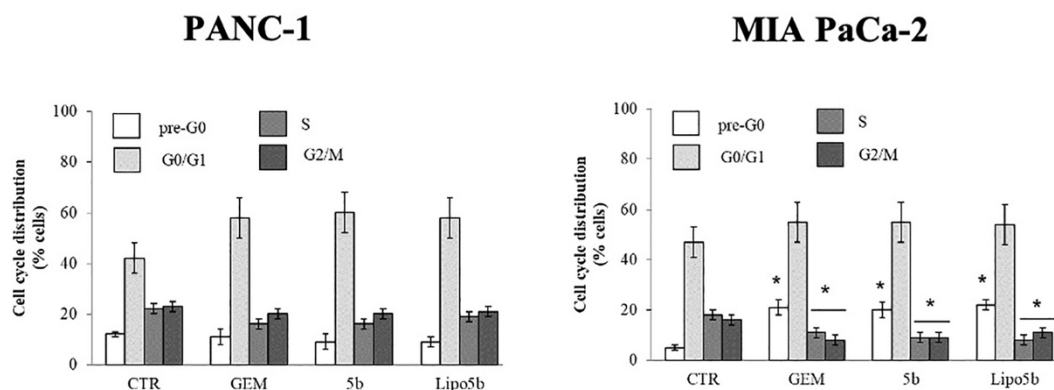


Figure 13. Distribution of the cell cycle phases after cell treatments with 100  $\mu$ M GEM, 5b or Lipo 5b for 48h. Measurements were performed in triplicate and data are presented as means  $\pm$  SD ( $n = 3$ ). Student's *t*-test: \* $p < 0.05$  GEM, 5b or Lipo 5b versus CTR.

#### 8.1.5 The intracellular release of NO by 5b or Lipo 5b is determinant to increase their cytotoxic effect

We functionally investigated the role of NO released by 5b and Lipo 5b on GEM-R PANC-1 cell growth inhibition. First of all, we analyzed the effective enhancement of the intracellular NO level after cell treatment with GEM, 5b or Lipo 5b, in the absence or presence of the NO scavenger PTIO or the nitric-oxide synthase (NOS) inhibitor L-NAME. Figure 7A shows that GEM treatment slightly increased the level of NO, which was completely reverted by L-NAME, in accordance with the previous observation that GEM triggered the NOS pathway in breast cancer cells.<sup>102</sup> Moreover, we demonstrated that 5b and Lipo 5b further enhanced the intracellular NO level, which was strongly reverted by PTIO, suggesting that NO increase by 5b or 5b encapsulated in liposomes is mainly due to the intracellular release of NO by the pro-drug rather than determined by the endogenous NO production induced by NOS pathway stimulation. Functionally,

we demonstrated that apoptosis (Figure 7B) and cell growth inhibition (Figure 7C) by 5b and Lipo 5b is recovered by PTIO, indicating a role of NO released by the pro-drug on the acquisition of chemosensitivity to GEM in GEM-R PANC-1 cells.

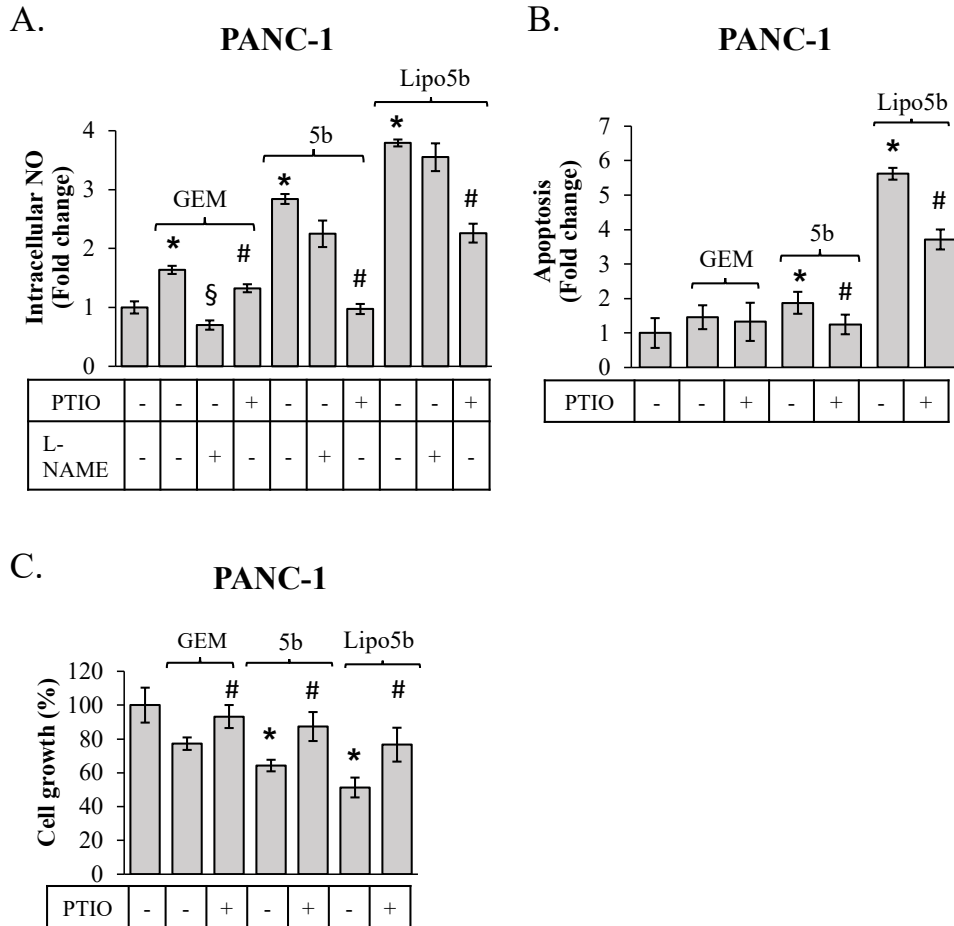


Figure 14. Detection of intracellular NO amount after GEM, 5b or Lipo 5b treatments and its role in cytotoxicity. PANC-1 cells were treated for 48h with GEM, 5b, Lipo 5b or PTIO 100  $\mu$ M; L-NAME 1mM. Intracellular NO (A), apoptosis (B) and cell growth (C) were analyzed as reported in the Experimental Section. Measurements were performed in triplicate and data are presented as means  $\pm$  SD ( $n = 3$ ). Student's t-test: \* $p < 0.05$  GEM, 5b or Lipo 5b versus CTR; § $p < 0.05$  GEM + L-NAME versus GEM; # $p < 0.05$  GEM, 5b or Lipo 5b + PTIO versus GEM, 5b or Lipo 5b, respectively.

#### 8.1.6 MRP5 nitration by 5b or Lipo 5b confers chemosensitivity to GEM-R cells

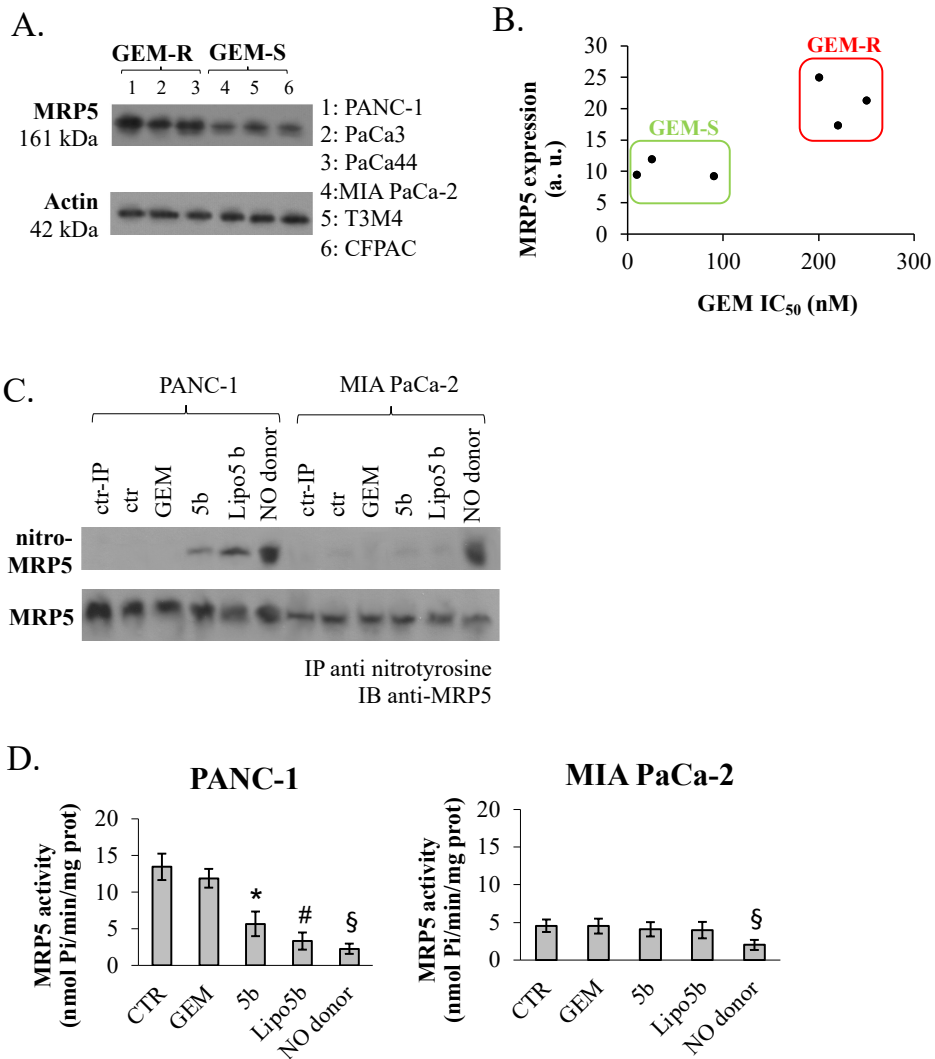
MRP5 pump, which expression and activity is increased in PDAC cells<sup>38</sup>, is known to reduce the cytotoxic effect of GEM treatment<sup>38, 40, 103, 104</sup>. Moreover, different studies reported that the nitration of MRP transporters impair their catalytic efficiency.<sup>105, 106, 107</sup>. Thus, we tested whether NO released by 5b pro-drug may nitrate the MRP5 pump affecting its activity.

First, we analyzed the expression levels of MRP5 protein in a panel of six PDAC cell lines. Notably, Figure 15A and B shows that MRP5 is more expressed in PDAC cell lines with higher IC50 value for GEM (PANC-1, PaCa3 and PaCa44), as compared to PDAC cell lines with lower IC50 value for GEM (MIA PaCa-2, T3M4, CFPAC), suggesting the involvement of MRP5 expression in GEM chemoresistance. Importantly, with the help of our collaborators, we also demonstrated by immunoblotting that treatments with 5b nitrated the MRP5 pump in GEM-R PANC-1 cells, characterized by high expression levels of this protein.

By contrast, we did not detect any nitration in GEM-S MIA PaCa-2 cells, except in the case of NO donor (Figure 15C). Such different profile may be explained by the lower level of MRP5 in MIA PaCa-2 cells: in these conditions, only a strong NO releasing agent as SNAP<sup>90</sup> release sufficient amount of NO to produce a detectable nitration; the amount of NO released by 5b likely induces a nitration rate that is below the detection limit of immunoblot.

Furthermore, we also observed a stronger MRP5 nitration in PANC-1 cells treated with 5b encapsulated in liposomes, according to the increased uptake of the drug by liposomes delivery (Figure 15C). This post-translational modification of the MRP5 pump is likely due to the intracellular release of NO by the pro-drug. We further investigated the impact of this post-translation modification on the activity of the MRP5 pump. Figure 15D shows that, in line with the different expression levels, the basal endogenous activity of MRP5 is higher in PANC-1 cells than in MIA PaCa-2 cells and that it is strongly inhibited after treatment with 5b or Lipo 5b in GEM-R PANC-1 cells. In MIA PaCa-2 cells, on the other hand, the activity of the MRP5 pump is not affected by the pro-drug, in line with the absence of protein nitration. Finally, to demonstrate the role of MRP5 inhibition in the

acquisition of sensitivity to GEM we knocked-down MRP5 expression by shRNA for MRP5. MRP5 knock-down strongly enhanced the sensitivity of PANC-1 cells to GEM, 5b or Lipo 5b (Figure 15E). Altogether these data strongly suggest the involvement of NO-mediated nitration in the inhibitory effect of MRP5 activity and in the enhanced cytotoxic effect of 5b pro-drug, as compared to the standard drug GEM, in chemoresistant PDAC cells. Finally, encapsulation of the pro-drug is a valuable approach to further enhance 5b uptake and its anti-tumoral effects in PDAC cells.



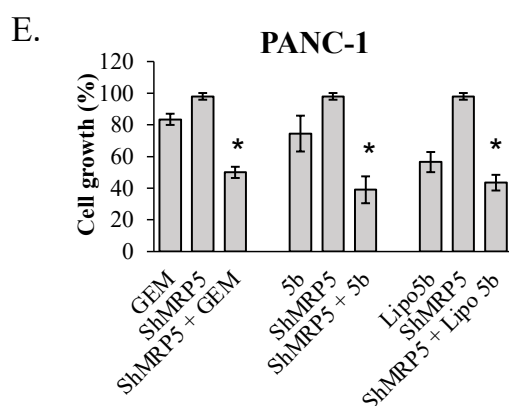


Figure 15. MRP5 inhibition sensitizes PANC-1 cells to the treatment with GEM, 5b or Lipo 5b. (A) Western Blotting analysis of MRP5 expression in GEM-R and GEM-S PDAC cell lines (A) and its relation with GEM IC<sub>50</sub> values (B). Cells were treated with 100  $\mu$ M GEM, 5b or Lipo 5b for 48 h. NO donor: SNAP 100  $\mu$ M. Cell protein extracts were used for MRP5 detection, nitration (C) and activity (D) as described in the Experimental Section. Student's t-test: \* $p < 0.05$  5b versus GEM; # $p < 0.05$  Lipo 5b versus 5b; § $p < 0.05$  NO donor versus CTR. (E) Cell growth analysis after MRP5 knock-down (by using shRNA#2) in the absence or presence of 100  $\mu$ M GEM for 72 h. Measurements were performed in triplicate and data are presented as means  $\pm$  SD ( $n = 3$ ). Student's t-test: \* $p < 0.05$  shMRP5 + GEM versus GEM; shMRP5 + 5b versus 5b; shMRP5 + Lipo 5b versus Lipo 5b



## 8.2 New selective and reversible MAGL inhibitor synergizes with GEM and represents a promising anticancer agent for the treatment of pancreatic cancer

### 8.2.1 MAGL expression in pancreatic cancer correlates with a poor overall survival

MAGL is overexpressed in different tumor types, including pancreatic adenocarcinoma (PAAD) as demonstrated by the analysis of RNA sequencing expression data of 179 pancreatic tumors and 171 normal pancreatic samples from the TCGA and GTEx projects<sup>108</sup> and reported in Figure 16A. Applying the online genomics and visualization platform R2 (<http://r2.amc.nl>) on the pancreatic adenocarcinoma TCGA dataset (178-rsem-tcgars), 57 patients were classified with high MAGL mRNA expression, 89 with a low MAGL mRNA expression while 32 samples were excluded due to missing survival data. In the computed Kaplan-Meier curve (Figure 16B), it is shown that a high MAGL mRNA level is significantly ( $p=0.007$ ) correlated with a poor overall survival compared to a low expression. During my experience abroad in Giovannetti's laboratory at Cancer Center Amsterdam (VU University Medical Center) we considered two primary pancreatic cancer cell lines as our models (PDAC2 and PDAC3) since next-generation RNA sequencing (NGS) data from the laboratory showed that MAGL mRNA is differently expressed between the two cell lines, with the highest Fragments Per Kilobase Million (FPKM) score in PDAC3 cells (Figure 16C), which originated from the most clinically aggressive tumor<sup>109</sup>.

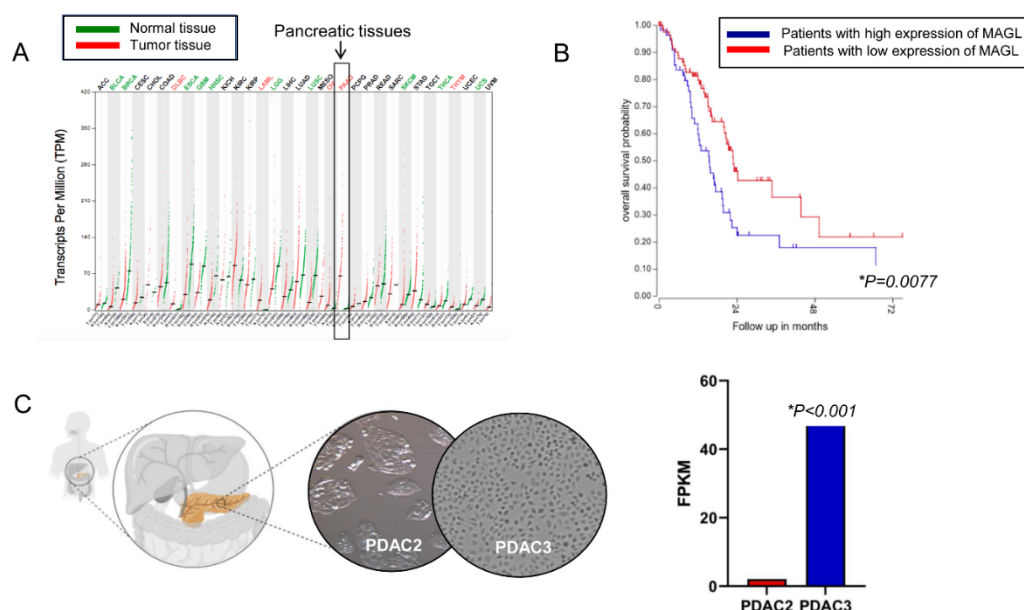


Figure 16. *MAGL* gene expression levels. (A) *MAGL* mRNA is more expressed in cancer tissues than in normal tissues (<http://gepia.cancer-pku.cn/detail.php?gene=MAGL>). Pancreatic cancer tissues are amongst the tumor tissues with the highest expression levels of *MAGL* (B). *MAGL* mRNA expression is a prognostic factor in pancreatic cancer. (C) Two primary pancreatic cancer cell cultures (PDAC2 and PDAC3) originated from patients undergoing surgery for pancreatic cancer showed significantly different expression levels of *MAGL* mRNA.

### 8.2.2 Novel *MAGL* inhibitor show higher cytotoxic effect on aggressive PDAC primary culture

Compound 13, a novel selective and reversible *MAGL* inhibitor, was synthesized by collaborators from the University of Pisa. Thus, we tested it in antiproliferative activity assays on different pancreatic ductal adenocarcinoma cancer cells, including SUI-2 immortalized cell line, PDAC2 and PDAC3 primary cell cultures, and HPNE non-tumoral pancreatic cell line. PDAC2 and PDAC3 cell cultures were chosen as cellular models because they maintain the same metastatic, genetic and histopathological features of the primary tumor.

PDAC2, PDAC3 and SUI-2 cells showed different sensitivities to compound 13 (Figure 17A). SUI-2 and PDAC2 cells, despite being immortalized and primary

cells culture, show a similar sensitivity. More specifically, the IC<sub>50</sub> values of SUI-2 and PDAC2 were 11.19 and 12.61 μM, respectively. H PDAC3 cells were slightly more sensitive to MAGL inhibitor 13 with an IC<sub>50</sub> value of 7.25 μM, in line with the higher expression of MAGL in PDAC3 compared to PDAC2 primary cell culture. JZL184 was used as reference compound since it represents an important milestones in the development history of MAGL irreversible inhibitors<sup>110</sup>. All the tested cells were not sensitive to JZL184 as demonstrated by the inhibition of cell growth curves, showing more than 50% of the cells still proliferating after exposure to 20 μM (Figure 17B). Of note, the immortalized pancreatic ductal normal cells were not sensitive to both compound 13 and JZL184.

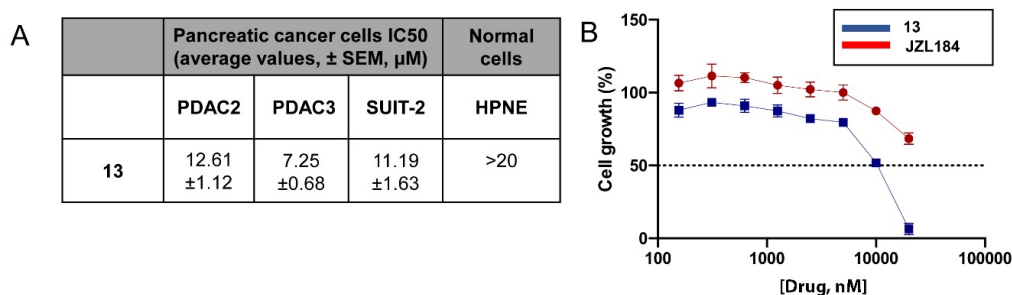


Figure 17. Antiproliferative effects of MAGL inhibitor 13. (A) IC<sub>50</sub> of compound 13 in different pancreatic cancer models and in the immortalized ductal cells HPNE. (B) Representative curves of PDAC3 cells growth inhibitory effects of 13 and JZL184, as control. Measurements were performed in triplicate and data are presented as means ± SEM.

### 8.2.3 In more aggressive primary cell model, inhibitor 13 increases apoptosis, and the effect is higher when combined with GEM

We evaluated apoptosis induction by compound 13, and compared its pro-apoptotic effect with GEM, as standard treatment, which has IC<sub>50</sub> values in the nanomolar range, as reported in a previous collaboration study between the same groups in Pisa and Amsterdam<sup>111</sup>. The effects of compound 13 was further evaluated by specific apoptotic assays. In particular, the Annexin-V staining showed that the inhibitor strongly enhanced apoptosis induction in PDAC3 cells (Figure 18A).

Remarkably, this compound was able to significantly increase apoptosis induction compared to untreated cells. GEM has a similar effect and the combination led to an additive effect. Similar results were observed in PDAC2 cells (i.e., apoptosis fold induction/change of approximately 4, 5 and 9 after treatment with 13, GEM and their combination). Moreover, we demonstrated that the apoptotic response of both PDAC3 and PDAC2 cells after exposure to compound 13 was associated to the concomitant stimulation of Caspase-3 (Figure 18B). Indeed, our immunoassay measured significantly higher levels of active Caspase-3 in PDAC3 cells treated with compound 13 or GEM compared to untreated cells. PDAC2 cells showed similar results with slightly lower levels of active Caspase-3 (0.35 ng/ml, 0.88, and 1.12 in untreated, GEM-treated, and 13-treated cells, respectively).

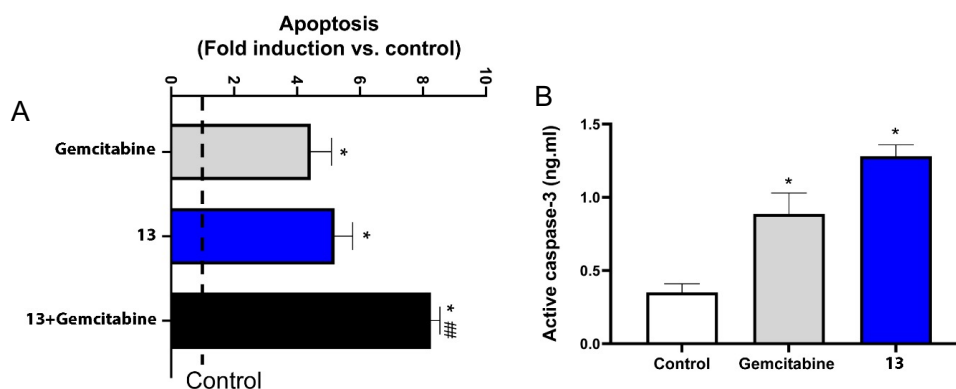


Figure 18. Pro-apoptotic effects of MAGL inhibitor 13. (A) Induction of apoptosis and (B) levels of active Caspase-3 in PDAC3 cells treated with compound 13 or GEM for 72 hours, compared to control/untreated cells (value=1, as illustrated by the dashed line). Measurements were performed in triplicate and data are presented as means  $\pm$  SEM. \* $p < 0.05$  versus control; # $p < 0.05$  versus gemcitabine.

#### 8.2.4 Inhibitor 13 shows anti-migratory effect in PDAC3

The effect of compound 13 on cell migration was investigated by wound-healing assay. In PDAC3 cells (Figure 19A), treatment with 13 induced a significant reduction of migration compared to control cells treated with DMSO.

In the PDAC3 cells (Figure 19A),  $59 \pm 8\%$  of the scratch area was closed after 20 hours when treated with 0.1% DMSO (control). After treatment with JZL184  $50 \pm 6\%$  of the scratch was closed, while compound 13 induced a significant reduction of migration, with  $38 \pm 6\%$  of the scratch closed (Figure 19B). Similarly, in PDAC2 the control showed  $70 \pm 3\%$  of gap closure. However, in these cell lines inhibitor 13 and JZL184 treatments resulted in a comparable migration with  $61 \pm 3\%$  and  $66 \pm 2\%$ , respectively.

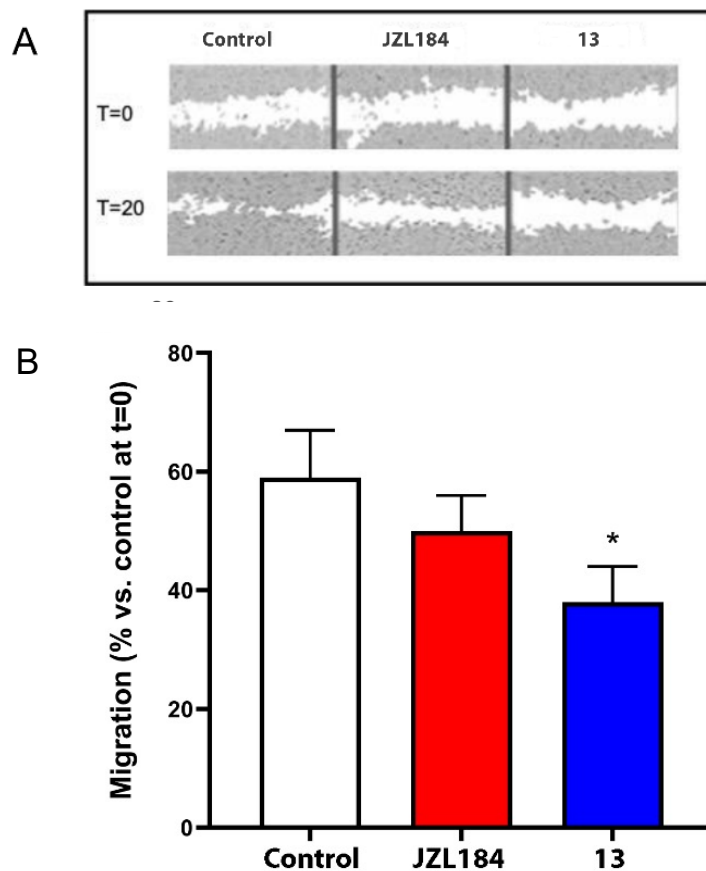


Figure 19. Anti-migratory effect of MAGL inhibitors. (A) Representative images of migration assay after 0 and 20 hours in PDAC3 cells. (B) Quantification of the wound-healing/migration assay on the PDAC3 cells 20 hours after scratch induction and treatment. The percentages of scratch closure for control, 13- or JZL184-treated cells were compared with one-way analysis of variance (ANOVA)/t-test. \* $p < 0.05$  versus control.

### 8.2.5 Synergistic interaction of compound 13 with GEM and potential mechanisms underlying its effects on apoptosis, migration, and potentiation of GEM activity

The pharmacological interaction of compound 13 and GEM was determined (Figure 20A) using fixed concentration values of compound 13 at IC<sub>25</sub> and IC<sub>50</sub>. The PDAC3 cells treated with GEM and inhibitor 13 at IC<sub>50</sub> showed synergy, whereas compound 13 at IC<sub>25</sub> was additive. The PDAC2 cells showed a slight synergy between GEM and compound 13 at IC<sub>50</sub> (CI, 0.76) and additive interaction with 13 at IC<sub>25</sub> (CI, 0.96).

To elucidate the previous data and investigate the mechanism of interaction, further studies focused on several potential cellular determinants and effectors of drug activities, such as the anti-apoptotic factor Bcl-2, the key matrix metalloproteinase 9 (MMP9), which promotes cell migration, and the main GEM transporter, the human equilibrative nucleoside transporter 1 (*hENT1*). As shown in Figure 20B, RT-PCR analyses demonstrated a slightly reduction of Bcl-2, and a significant reduction of MMP9 and increased expression *hENT1*.

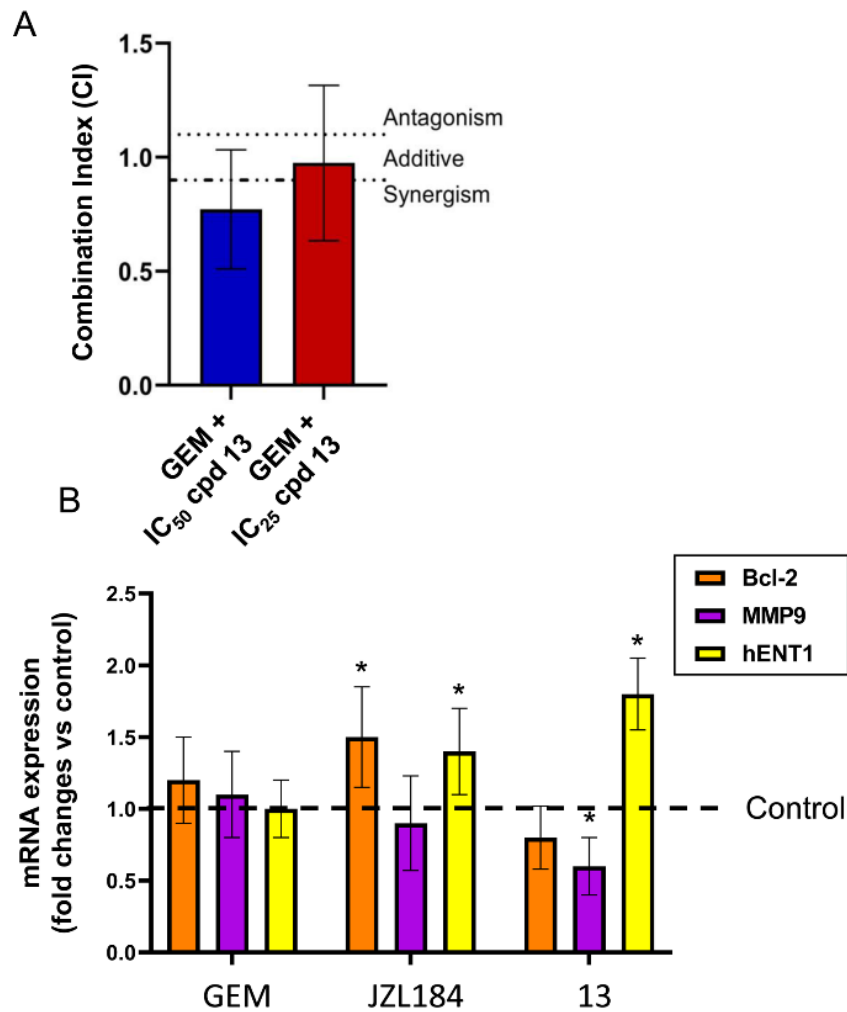


Figure 20. Combination assay and modulation of gene expression. (A) CI values of gemcitabine (GEM) combined with compound 13 at IC<sub>50</sub> and IC<sub>25</sub>. The upper line represents an antagonistic CI > 1.2, the lower bar represents a synergistic CI < 0.8. (B) This figure combines the results of different PCR experiments, evaluating the effect of GEM, 13 and JZL184 on potential determinants of apoptosis induction, migration, and synergistic interaction with gemcitabine compared to control/untreated cells (value=1, as illustrated by the dashed line). Measurements were performed in triplicate and data are presented as means ± SEM. \**p* < 0.05 versus control.

### 8.3 Mutant p53 R273H isoform supports MAGL overexpression in PDAC cells

#### 8.3.1 MGLL gene expression is higher in patients with mutated forms of TP53

Since mutations in tumor suppressor *TP53* are frequent in PDAC, and that mutant-p53 plays a role in lipid metabolism contributing to tumor progression<sup>54</sup>, we investigated a possible correlation between mutant-p53 and the expression level of MAGL.

Analyzing the previous mentioned cancer genomic TCGA data set on PDAC by cBioPortal for Cancer Genomics (<https://www.cbioportal.org>), out of 178 total patients 102 have mutations in *TP53*, 64 have no mutations, while 12 were excluded due to lack of information. In the computed plot “mRNA vs mut type” presented as Figure 21, *MGLL* level is significantly ( $p=0.0013$ ) higher in patients harboring mutations in *TP53* gene compared with those having no mutation.



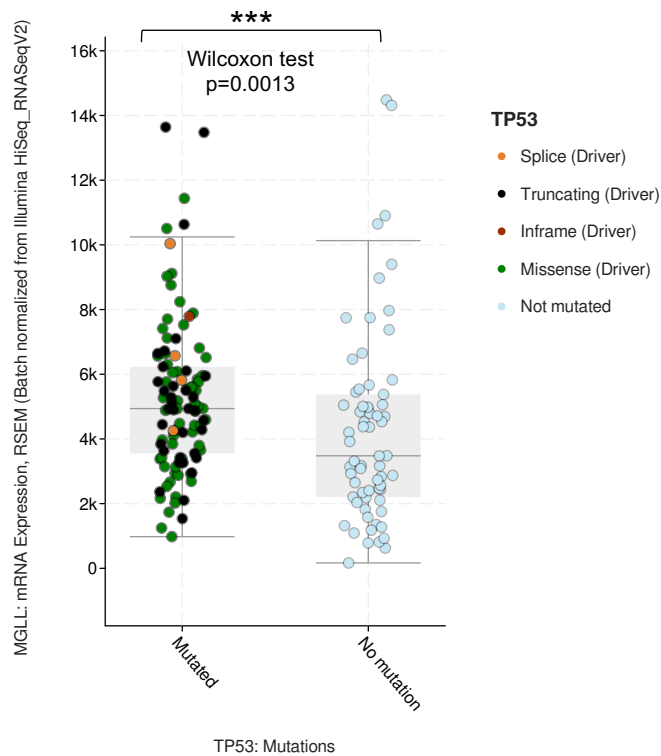


Figure 21. Higher levels of MAGL mRNA (*MGLL*) are correlated with mutations in *TP53* gene compared with those having no mutation.

### 8.3.2 Mutants TP53 enhanced *MGLL* gene expression in PDAC cell lines

Among the p53 GOF mutations, mutp53-R273H is a hot-spot mutant that affects the DNA-binding capacity of the protein, and which in our lab, has previously been shown to be particularly chemoresistant.<sup>112, 113</sup>

Here was evaluated whether p53, depending on its mutational status, could influence lipid metabolism toward a more aggressive tumor phenotype also through modulation of *MGLL* expression. Thus, we observed that knockdown of endogenous p53 in PANC-1 cells, harboring the R273H mutation of p53, inhibited *MGLL* expression (Figure 22A). Furthermore, exogenous overexpression of the same p53-mutant in AsPC-1, a p53-null PDAC cell line, increased MAGL expression, whereas overexpression of WT-p53 decreased it (Figure 22B).

To investigate whether this induction of *MGLL* by mutated p53 was mutant specific, we silenced the exogenous R248W hot-spot mutant in the MIA PaCa-2 cell line (Figure 22C). Also in this model, *MGLL* expression is inhibited by knockdown of p53.

These data support a direct role of mutant p53 in *MGLL* induction.

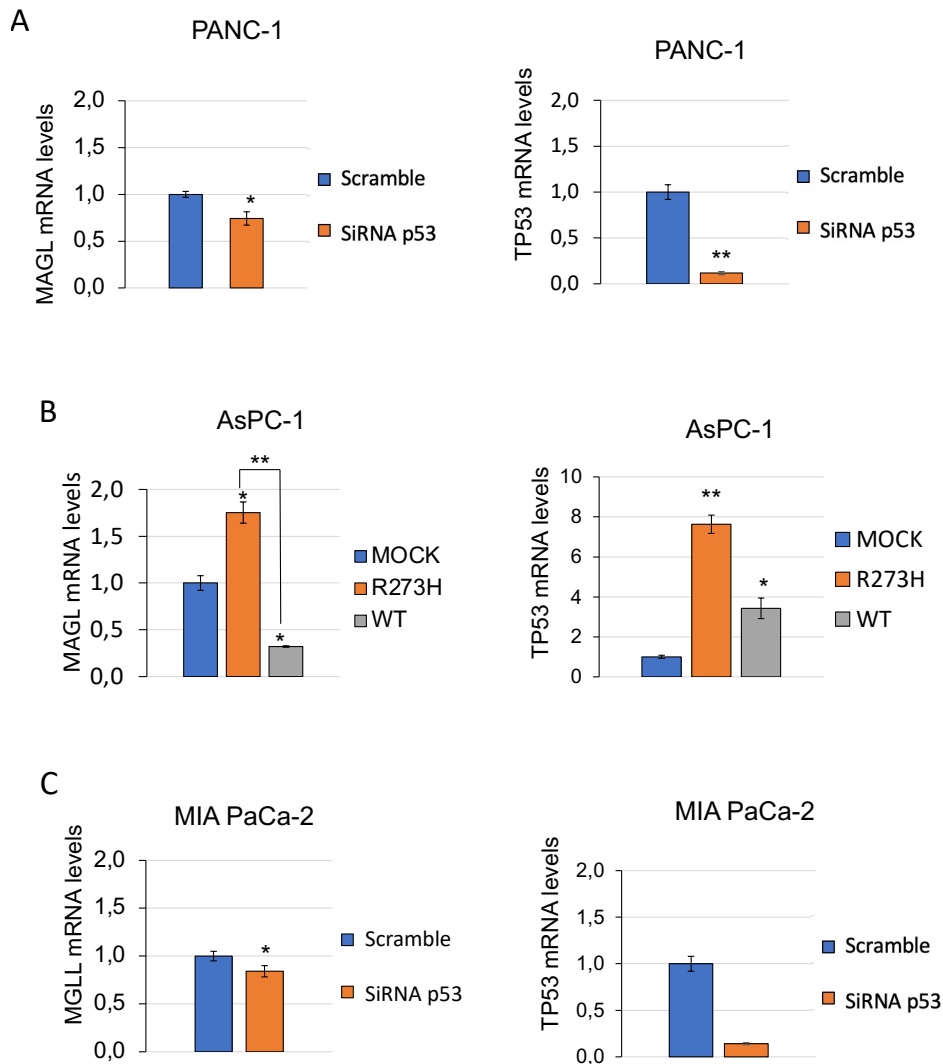


Figure 22. *MGLL* gene expression levels are modulated by p53: it is increased by mutR273H and inhibited by wt p53. (A) *MGLL* mRNA levels are decreased in PANC-1 cell line (p53 R273H mutated) after the knockdown of p53. (B) In AsPC-1 cell line (p53-null) overexpressed mutp53-R273H increases levels of *MGLL* mRNA, on the contrary wt p53 decrease *MGLL* gene expression. (C) As in PANC-1, *MGLL* mRNA levels in MIA PaCa-2 (p53 R248W mutated) after p53 silencing.

*p53 levels in each cell line are shown as proof of a correct occurred overexpression or silencing.*

*Measurements were performed in triplicate and data are presented as means  $\pm$  SD (n = 3).*

*Student's t-test: \*p < 0.05, \*\*p<0.01.*

### 8.3.3 Chemical inhibition of MGLL gene counteracted mutp53-dependent hyperproliferation

After demonstrating that mut-p53 correlates with MAGL expression, we investigated whether chemical inhibition of MGLL gene could counteract mutp53-dependent hyperproliferation.

First, we analyzed the antiproliferative effect of compound 13, described and tested in the previous part of this study as a new potent MAGL inhibitor, in PDAC cells focusing on comparing its effect in cells endogenously expressing mutp53 with p53-null cell line. In Figure 23, were reported the effects of increasing concentrations of inhibitor 13 in PANC-1, MIA PaCa-2 and AsPC-1 cell lines. Although the inhibitor has an antiproliferative effect even in cells where p53 is absent (AsPC-1), its IC<sub>50</sub> is reached at lower concentrations in GOF mutp53-expressing PANC-1 and MIA PaCa-2 cell lines.

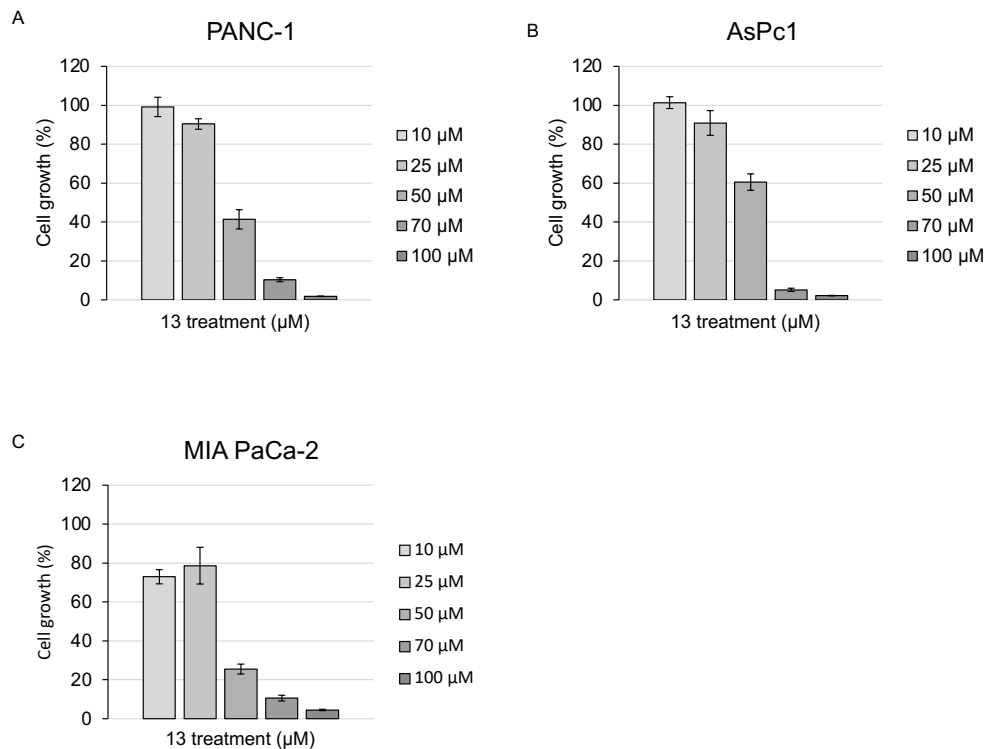


Figure 23. Effects of 48h treatment with MAGL inhibitor 13 at increasing concentration in our PDAC cell line models. Compound 13 reduces more cell growth in cells with mutated p53 than in cells not expressing p53. Measurements were performed in triplicate and data are presented as means  $\pm$  SD ( $n = 3$ ).

We investigated the link between cell proliferation and p53 mutational status by transfecting AsPC-1 and PaCa3 with wt and mutp53. In AsPC-1 transfected with R273H mutp53 (Figure 24A), treatment with compound 13 significantly decreased cell proliferation compared with untreated cells. Furthermore, compound 13 significantly counteracted hyperproliferation given by mutp53 showing a significant higher cytotoxic effect in mutated cells compared with mock-cells after the same treatment.

In PaCa3 cell line (Figure 24B), the exogenous overexpression of wt p53 shows a slightly lower response to inhibitor 13 treatment compared to mock. The analysis of the effect of mutp53 R273H in the same cell line, revealed the “negative dominant” effect of mutp53 and, in this setting, compound 13 showed a significant higher inhibition of cell growth compared to cells overexpressing the wt form.

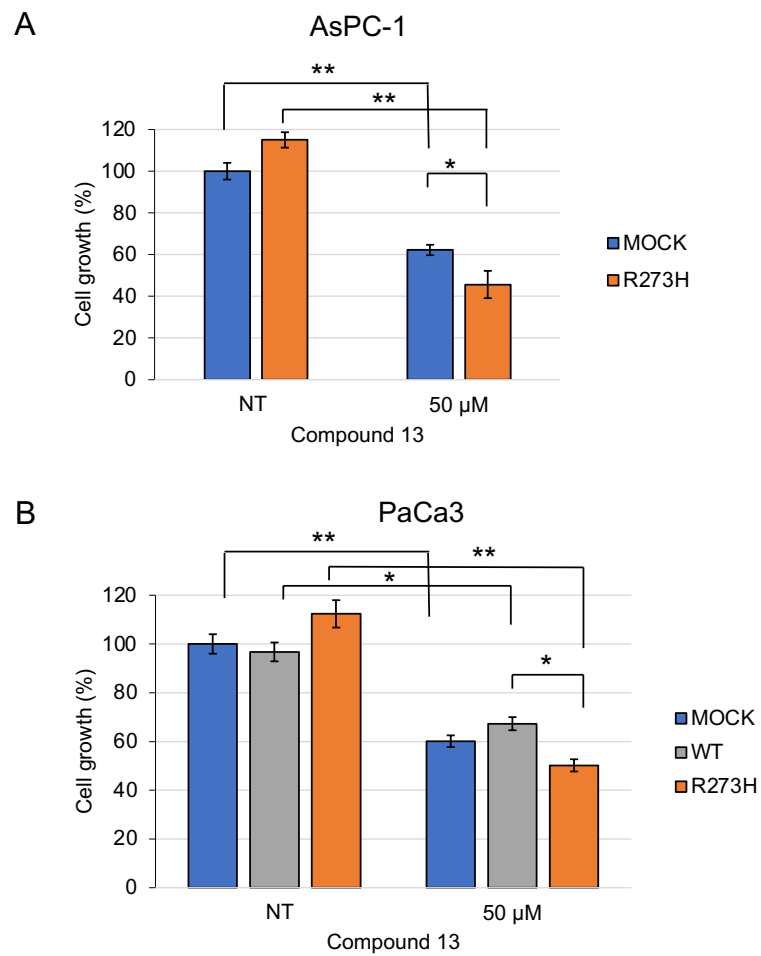


Figure 24. Compound 13 is more cytotoxic in cells overexpressing mutp53 R273H. Anti-proliferative effect of MAGL inhibitor 13 in AsPC-1 cell line after overexpression of mut-p53 R273H (A) and in PaCa3 cell line after overexpression of wt p53 or mutp53 R73H (B). Cells were treated for 48h. Measurements were performed in triplicate and data are presented as means  $\pm$  SD ( $n = 3$ ). Student's t-test: \* $p < 0.05$ , \*\* $p < 0.01$ .

#### 8.3.4 Cross-talk between p53 and NF- $\kappa$ B in the regulation of MAGL

In order to investigate the molecular basis of MGLL gene regulation, we analyzed MAGL promoter sequence (Figure 25A).

As we reported in a previous review, NF- $\kappa$ B, being involved in oncogenic program, is modulated by GOF mutant p53 in different tumors.<sup>20</sup>. Indeed, the induction of inflammatory signals by NF- $\kappa$ B increases levels of reactive oxygen species (ROS) to promote tumor progression.<sup>20</sup>.

Thus, applying PROMO (Version 3.0.2) online virtual laboratory for the study of transcription factor binding sites in DNA sequences (<http://alggen.lsi.upc.es>) on MAGL promoter, we determined whether NF- $\kappa$ B could be a predicted transcription factor. Furthermore, we also investigated a possible interaction between wt p53 and MAGL promoter. As shown in Figure 25B, NF- $\kappa$ B can interact with the promoter of MAGL, as well as p53. Of note, in line with opposite regulation on MAGL, they are competitors in the same sequence section. So, the hypothesis is that p53 wt normally is able to prevent NF- $\kappa$ B binding by not activating or inhibiting the gene. On the other hand, the mutation on p53 compromises direct binding but allows to recruit NF- $\kappa$ B to the promoter. In this way, GOF mutp53 could overexpress MAGL to generate a signaling of tumor progression.

**A**

Origin 1

GGAGAGCCTG	CCGGTGGGAG	CTGGAAGCAG	GCTCCCGGCT	GAGCGCCCCA
GCCCGAAAGG	CAGGGTCTGG	GTGCGGGAAG	AGGGCTCGGA	GCTGCCTTCC
TGCTGCCTTG	GGCCCGCCCA	GATGAGGGAA	CAGCCCGATT	TGCCTGGTTC
TGATTCTCCA	GGCTGTCGTG	GTTGTGGAAT	GCAAACGCCA	GCACATAATG
GAAACAGGAC	CTGAAGACCC	TTCCAGCATG	CCAGAGGAAA	GTTCCCCAG
GCGGACCCCG	CAGAGCATTG	CCTACCAGGA	CCTCCCTCAC	CTGGTCAATG
CAGACGGACA	GTACCTCTTC	TGCAGGTAAT	GGAAACCCAC	AGGCACACCC
AAGGCCCTCA	TCTTTGTGTC	CCATGGAGCC	GGAGAGCACA	GTGGCCGCTA
TGAAGAGCTG	GCTCGGATGC	TGATGGGGCT	GGACCTGCTG	GTGTTCCGCC
ACGACCATGT	TGGCCACGGA	CAGAGCGAAG	GGGAGAGGAT	GGTAGTGTCT
GACTTCCACG	TTTTCGTCAG	GGATGTGTTG	CAGCATGTGG	ATTCCATGCA
GAAAGACTAC	CCTGGGCTTC	CTGTCTTCTT	TCTGGGCCAC	TCCATGGGAG
GCGCCATCGC	CATCCTCACG	GCCGCAGAGA	GGCCGGGCCA	CTTCGCCGGC
ATGGTACTCA	TTTCGCCTCT	GTTTCTTGCC	AATCCTGAAT	CTGCAACAAC
TTTCAAGGTC	CTTGCTGCGA	AAGTGCTCAA	CCTTGTGCTG	CCAACCTTGT
CCCTCGGGCC	CATCGACTCC	AGCGTGCTCT	CTCGGAATAA	GACAGAGGTC
GACATTTATA	ACTCAGACCC	CCTGATCTGC	CGGGCAGGGC	TGAAGGTGTG
CTTCGGCATC	CAACTGCTGA	ATGCCGTCTC	ACGGGTGGAG	CGCGCCCTCC
CCAAGCTGAC	TGTGCCCTTC	CTGCTGCTCC	AGGGCTCTGC	CGATCGCCTA
TGTGACAGCA	AAGGGCCCTA	CCTGCTCATG	GAGTTAGCCA	AGAGCCAGGA
CAAGACTCTC	AAGATTTATG	AAGGTGCCTA	CCATGTTCTC	CACAAGGAGC
TTCTGAAATG	CACCAACTCC	GTCTTCCATG	AAATAAACAT	GTGGGTCTCT
CAAAGGACAG	CCACGGCAGG	AACTGCGTCC	CCACCCTGAA	TGCATTGGCC
GGTGCCCGGC	TCATGGTCTG	GGGGATGCAG	GCAGGGGAG	GGCAGAGATG
GCTTCTCAGA	TATGGCTTGC	CAAAAAAAAA	AAAAAAAAAAA	AATCAGAAAT
TGGAGAAATC	CTTAGCACAA	TTTTCTAAAA	AATAACAGAC	ATTTTTGTTA
TACATTAGAC	TATCAGACAC			

+1261

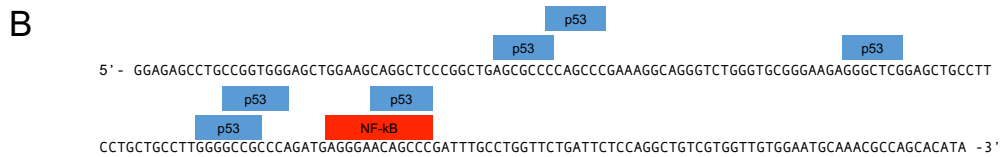


Figure 25. Human MAGL gene promoter. (A) MAGL gene nucleotide sequence. In red is highlighted the sequence of the promoter, while the MAGL coding DNA sequence is in black. (B) NF-κB and p53 binding sites on MAGL promoter sequence. Factors are predicted within a dissimilarity margin less or equal than 15%.

## 9 DISCUSSION

Although research efforts on PDAC have been steadily increasing over the years, improving patient survival remains a big challenge. The main difficulty in treating this cancer type is the resistance to the existing therapies, whose efficiency still remains too low. Chemoresistance can act at different levels: modulating the expression of drug importer and exporter, altering drug targets, increasing repair of drug-induced DNA damage, evading apoptosis, and stimulating abnormal autophagy.<sup>30</sup> Moreover, a fundamental component of acquired resistance is due to the molecular mutations developed by the tumor and its microenvironment, so the patients become differentially responsive to the therapy<sup>30, 113</sup>. Mutations lead to general metabolic remodeling within the tumor cell, which in turn activates abundant stromal cells in the microenvironment to exchange metabolites thus fueling tumor progression.<sup>114</sup> In tumor cells, this metabolic change also occurs with the increase of antioxidant pathways, and the activation of alternative energy pathways. Indeed, a dysregulated lipid metabolism is related to tumor survival and progression as cancer cells need to generate building materials for membrane, lipid second messenger and energy supply. Moreover, lipid metabolites can be secreted to create a tumor-favoring immune microenvironment<sup>115</sup>.

Important mutations in the context of chemoresistance are those in the *TP53* gene, particularly GOF mutations, which result not only in the loss of p53 tumor suppressor function but also in the acquisition of new oncogenic functions that affect the sensitivity of tumor cells to chemotherapeutics, as previously demonstrated in our laboratory<sup>112</sup>.

Since FDA approval, GEM has remained a cornerstone of PDAC chemotherapy especially as a first-line drug for patients with advanced staged, despite not being a completely effective and decisive treatment. Most studies examining chemoresistance in advanced pancreatic cancer focused on GEM, as data on the action of other drugs remain preliminary<sup>116</sup>. In addition to the physical barrier caused by the desmoplastic reaction, the effect of GEM is compromised by poor membrane permeability, increased transporters for its extrusion, rapid clearance in the blood due to deoxycytidine deaminase (CDA), and changes in various enzymes



that regulate its metabolism. All these factors contribute to chemoresistance at the molecular level<sup>117</sup>.

In the effort to counteract chemoresistance, in this study, we designed and analyzed different approaches to specifically target the more resistant PDAC tumor forms. In the first part, we potentiated the existing standard therapy GEM to overcome the main mechanisms of resistance that act directly against the drug molecule or its active metabolites, preventing its accumulation or function<sup>91</sup>.

Thus, seven new pro-drugs derived from GEM and added with NO-donor moieties were synthesized by our collaborators, in order to achieve several therapeutic advantages: (1) to protect the pro-drug from CDA-catalyzed inactivation of cytidine into uracil, thus improving its metabolic stability<sup>118</sup>; (2) to confer a more lipophilic characteristic to the pro-drug for its efficient encapsulation in liposomes, which cannot be done with standard GEM<sup>119</sup>; (3) to release NO into cells through enzymatic pathways so as to have greater stability in the plasma to reach the tumor cells. Indeed it has been reported that high intracellular concentrations of NO can produce anti-tumor effects shifting the balance towards cell death<sup>83</sup>. As evident from the growing number of pre-clinical studies and clinical trials regarding NO/NO-donors based anticancer therapy<sup>84</sup>, NO sensitizes cancer cells to the chemotherapeutic drugs treatment<sup>97</sup>. This concept was also previously demonstrated by our collaborators for doxorubicin drug in colon cancer cells<sup>90</sup>. Among the seven new NO-GEMs, we selected 5b displaying a more evident effect in GEM-R cells. In order to bypass the previous mentioned difficulty of GEM uptake in PDAC cells, 5b was encapsulated in liposomes, favoring drug delivery as revealed by the stronger intracellular accumulation of the drug after cell treatment with Lipo 5b, as compared to the non-encapsulated 5b pro-drug. Intriguingly, 5b and especially Lipo 5b enhanced the apoptosis level in GEM-R cells. These data were supported also by the increased expression level of the pro-apoptotic protein Bim in PANC-1 cells treated with 5b or Lipo 5b compared with standard GEM treatment. Bim is a member of the Bcl-2 family that promotes apoptosis through the mitochondrial intrinsic pathway<sup>120</sup> and whose expression is often suppressed in cancer cells, allowing tumor progression and metastasis.

NO released by 5b plays a fundamental role in decreasing cell growth and increasing apoptosis<sup>91</sup>. Indeed, we have shown that cell growth is recovered, concomitant with the decrease in apoptosis stimulus, when the increase in intracellular NO is counteracted with the NO scavenger, PTIO. The effect of NO released into the cells was further studied by investigating the involvement of MRP5 tyrosine nitration, leading to its reduced activity and therefore to increased intracellular GEM concentration. Given that nitration is promoted by NO-dependent oxidative processes induced by NO release or peroxynitrite-derived radicals and that GEM induces mitochondrial superoxide ion production<sup>121</sup>, the nitration reaction may be caused by ONOO- formed due to NO release by 5b. In MRPs, a nitration on tyrosine is commonly associated to a reduction of the catalytic efficiency of the transporters<sup>107,105</sup>. Interestingly, the MRP5 pump confers resistance to the treatment of the cells with GEM<sup>40</sup> and it is more expressed in GEM-R, as compared to GEM-S PDAC cell lines. Our data suggest that MRP5 pump is nitrated and inhibited by NO released by 5b and especially by Lipo 5b. In this way we obtained a decrease in the ATPase activity of MRP5 that can result in a decreased efflux of GEM. Thus, higher intracellular accumulation of GEM enhanced its anti-tumor effects<sup>91</sup>.

In the second part of this study, we targeted chemoresistance in a different way. We focused on molecular targets directly involved in the metabolic reprogramming of the tumor cell in order to identify new therapeutic strategies.

Although less studied than the Warburg effect and glutamine metabolism, in the last decade lipid metabolism rewiring has attracted increasing interest and now it is considered one of the most prominent metabolic alterations in cancer.<sup>122</sup> Moreover, in PDAC, the altered lipid metabolism represents a mechanism of GEM resistance.<sup>75</sup>

MAGL is a promising therapeutic target in cancer, since Nomura et al. linked it to the production of oncogenic signaling lipids that promotes migration, invasion, survival, and *in vivo* tumor growth.<sup>123</sup> On the other hand, it is a therapeutic target in neurodegenerative and inflammatory diseases as the main enzyme of synthesis of the endocannabinoid 2-AG.<sup>124</sup> This makes it an even more attractive target

because a single inhibitory molecule could be used as a drug in different diseases representing also an economic advantage.

Thus, novel highly selective and reversible MAGL inhibitors were specially synthesized, from which compound 13 was selected as the most potent *in vitro*. Since MAGL is overexpressed in PDAC and considering that MAGL mRNA overexpression is a very important factor for patients' prognosis, its effect was tested in two different MAGL expressing cell models. PDAC2 (low MAGL level) and PDAC3 (high MAGL level) cell lines were also selected as they maintain the same metastatic, genetic, and histopathological features of the primary tumor, thus, representing an important tool for the experimental testing of anti-cancer agents. Compound 13 was more effective than the standard inhibitor JZL184 and it showed the best antiproliferative effect in the more aggressive primary cell type PDAC3, in which MAGL is highly expressed. Previous studies suggested that inhibition of MAGL might increase apoptosis and tumor cell sensitivity to chemotherapy<sup>125, 61</sup>. Intriguingly, in PDAC3, compound13 not only induced more apoptosis compared to a standard PDAC chemotherapy as GEM, but also sensitized cells to treatment with GEM by further inducing apoptosis. In support of these data, the interaction between the two drugs proved to be additive or even synergistic by increasing the concentration of the inhibitor 13.

Furthermore, compound 13 showed the ability to affect the aggressiveness of PDAC by reducing the migratory capacity of the cells. It is well known that the early metastatic behavior of PDAC is responsible for the poor prognosis of this tumor, indeed the median survival for metastatic PDAC patients remains <1 year<sup>126</sup>. In addition, inhibitor 13 significantly reduced hENT1 expression, which is a potential predictive biomarker of GEM efficacy<sup>127</sup>, and gelatinase MMP9, which is involved in tumor infiltration and migration<sup>128,129</sup>. These data suggest that compound 13, could increase the concentration of GEM in cells by enhancing its anti-tumor effects and, on the other hand, counteract metastasis and tumor progression.

Interestingly, since MAGL is also involved in the endocannabinoid system hydrolyzing 2-Arachidonoylglycerol to arachidonic acid, thus MAGL blockade increasing the levels of 2-AG is able to reduce chemotherapy side effects such as

nausea and emesis. Indeed, 2-AG can interact with presynaptic CB-receptors leading to antinociceptive and anti-inflammatory effects.

Considering that the PDAC preclinical models we tested for this study share the same molecular and histopathological complexity of the tumor of origin and that this represents an important tool for the experimental testing of anti-cancer agents, all these results support the potential applicability to the clinical setting of this class of MAGL inhibitors.

Finally, in this study, we targeted PDAC chemoresistance by focusing on mutations that characterize tumor development and underlie innate drug resistance. Specifically, we analyzed GOF mutations in the p53 protein that acquire oncogenic functions making the tumor more aggressive and enhancing resistance to GEM, as already demonstrated by our laboratory<sup>113</sup>. It has long been known that different p53 mutations result in different resistance to therapy<sup>130</sup>; for example, the hot-spot mutation R273H renders the cells more resistant to GEM treatment than R175H mutation<sup>112</sup> and p53 helps accelerating lipid accumulation, which could further contribute to cancer progression<sup>54</sup>.

We found a correlation between MAGL gene expression levels and mutated p53 both from patient-derived data available in online databases and in our PDAC cell line models. Indeed, in our models, R273H mutp53 increases levels of MAGL mRNA, as we demonstrated by overexpressing mutant protein in p53-null AsPC-1 cells. Data was supported also by the inhibition of MAGL after the knockdown of endogenous R273H mutant p53 in Panc-1 cells. On the other side, overexpression of wt p53 in AsPC-1 showed the inhibition of MAGL gene expression. All together these results suggest a role for mutant p53 in the overexpression of MAGL in PDAC, potentially contributing to the development of an aggressive PDAC phenotype and to a poor clinical outcome.

Since in the previous part of this study, we demonstrated that MAGL inhibitor 13, is most effective in the primary PDAC cells expressing MAGL at higher levels, we tested the effect of the inhibitor in relation with mutp53. Compound 13 showed a higher effect in cell lines having mutated p53 than in p53-null. This was also confirmed after the overexpression of R273H mutp53 in AsPC-1. Intriguingly, in PaCa3 the antiproliferative effect of compound 13 is significantly higher when

mutp53 is overexpressed compared to the wt form. These data further support that mutp53 enhance MAGL gene expression and that inhibitor 13 is a good cytotoxic agent in more aggressive PDAC cell models counteracting the hyperproliferation induced by mutp53.

Moreover, to deeply investigate the role of p53 in the modulation of MGLL gene expression, we investigated the possible molecular mechanism. NF- $\kappa$ B and p53 were predicted to be a possible transcriptional factor for MAGL modulation. Indeed, it is known that NF- $\kappa$ B can be activated (or kept in an active status) by mutp53<sup>20</sup>. Thus, NF- $\kappa$ B may be recruited on MAGL promoter to induce its expression by GOF mutant p53 proteins. On the other hand, wt p53 may regulate MGLL gene expression inhibiting it through the bind competition with of NF- $\kappa$ B. Data shown together with other evidences in literature<sup>131</sup> suggest the crucial role of GOF p53 in enhancing tumor aggressiveness through a metabolic reprogramming. This thesis presents pre-clinical evaluations of different strategies to overcome chemoresistance that could be further investigated. Especially this last part, is clearly an ongoing study with a prediction that need to be confirmed by further analysis. For instance, we are planning to evaluate MAGL protein levels, in addition to gene expression, as a result of modulation by p53. We would confirm the correlation of mutp53 with NF- $\kappa$ B. Moreover, we thought to extend the analysis also to other missense mutations to investigate better if different mutations respond differently to inhibitor therapy.

## 10 CONCLUSIONS

Despite advances in understanding chemoresistance in pancreatic cancer, being multifaceted, finding an effective therapy is still challenging.

All together our data suggest different strategies to counteract chemoresistance in aggressive PDAC subtypes: overcoming drug resistance mechanisms using NO-GEM pro-drugs encapsulated in liposomes that block drug extrusion pumps sensitizing chemoresistant PDAC cells to GEM treatment or by inhibiting a key factor of dysregulated metabolism that support tumorigenesis. Using MAGL reversible inhibitors we increased the sensitivity of aggressive PDAC cells to GEM treatment. Furthermore, showing the role of *TP53* GOF mutations in orchestrating the lipid metabolic remodeling which promotes tumor aggressiveness, this thesis supports the importance of patient stratification and personalized medicine to ensure the most effective treatment.

## 11 BIBLIOGRAPHY

1. Bray F, Ferlay J, Soerjomataram I. Global Cancer Statistics 2018 : GLOBOCAN Estimates of Incidence and Mortality Worldwide for 36 Cancers in 185 Countries. 2018;394-424. doi:10.3322/caac.21492.
2. Carioli G, Malvezzi M, Bertuccio P, et al. European cancer mortality predictions for the year 2021 with focus on pancreatic and female lung cancer. *Ann Oncol.* 2021;32(4):478-487. doi:10.1016/j.annonc.2021.01.006
3. AIOM-AIRTUM. *I Numeri Del Cancro in Italia 2021.*; 2021.
4. Midha S, Chawla S, Kumar P. Modifiable and non-modifiable risk factors for pancreatic cancer : A review. *Cancer Lett.* 2016;381(1):269-277. doi:10.1016/j.canlet.2016.07.022
5. Maisonneuve P. Quarterly Medical Review Epidemiology and burden of pancreatic cancer. *Press Med.* 2019;(March):48: e113–e123.
6. Maisonneuve P. Epidemiology and burden of pancreatic cancer. *Press Medicale.* 2019;48(3P2):e113-e123. doi:10.1016/j.lpm.2019.02.030
7. Saiki Y, Horii A. Molecular pathology of pancreatic cancer. 2014;(October 2013):10-19. doi:10.1111/pin.12114
8. Grant TJ, Hua K, Singh A. Molecular Pathogenesis of Pancreatic Cancer. *Prog Mol Biol Transl Sci.* 2016;144:241-275.
9. Søreide K, Primavesi F, Labori KJ, Watson MM, Stättner S. Molecular biology in pancreatic ductal adenocarcinoma: implications for future diagnostics and therapy. *Eur Surg - Acta Chir Austriaca.* 2019;51(3):126-134. doi:10.1007/s10353-019-0575-z
10. Amrutkar M, Gladhaug IP. Pancreatic cancer chemoresistance to gemcitabine. *Cancers (Basel).* 2017. doi:10.3390/cancers9110157
11. Whatcott C, Posner R, Von Hoff D, al. et. Desmoplasia and chemoresistance in pancreatic cancer. In: *Transworld Research Network.* ; 2015:1-9. <https://www.ncbi.nlm.nih.gov/books/NBK98939/>.
12. Ebel ND, Zamloot V, Manuel ER. Targeting desmoplasia in pancreatic cancer as an essential first step to effective therapy. *Oncotarget.* 2020;11(38):3486-3488. doi:10.18632/oncotarget.27745
13. Liu J, Zhang C, Hu W, Feng Z. Tumor suppressor p53 and its mutants in cancer metabolism. *Cancer Lett.* 2015;356(2):197-203. doi:10.1016/j.canlet.2013.12.025
14. Li H, Zhang J, Tong JHM, et al. Targeting the oncogenic p53 mutants in colorectal cancer and other solid tumors. *Int J Mol Sci.* 2019;20(23).

doi:10.3390/ijms20235999

15. Zilfou JT, Lowe SW. Tumor suppressive functions of p53. *Cold Spring Harb Perspect Biol.* 2009;1(5):1-12. doi:10.1101/cshperspect.a001883
16. Boutelle AM, Attardi LD. p53 and Tumor Suppression: It Takes a Network. *Trends Cell Biol.* 2021;31(4):298-310. doi:10.1016/j.tcb.2020.12.011
17. Amelio I, Melino G. Context is everything: extrinsic signalling and gain-of-function p53 mutants. *Cell Death Discov.* 2020;6(1). doi:10.1038/s41420-020-0251-x
18. Stein Y, Rotter V, Aloni-grinstein R. Gain-of-Function Mutant p53 : All the Roads Lead to Tumorigenesis. *Int J Mol Sci.* 2019;20(24):6197.
19. Bullock AN, Fersht AR. Rescuing the function of mutant p53. *Nat Rev Cancer.* 2001;1(1):68-76. doi:10.1038/35094077
20. Cordani M, Butera G, Pacchiana R, et al. Mutant p53-associated molecular mechanisms of ROS regulation in cancer cells. *Biomolecules.* 2020. doi:10.3390/biom10030361
21. Cordani M, Pacchiana R, Butera G, D'Orazi G, Scarpa A, Donadelli M. Mutant p53 proteins alter cancer cell secretome and tumour microenvironment: Involvement in cancer invasion and metastasis. *Cancer Lett.* 2016. doi:10.1016/j.canlet.2016.03.046
22. Singh RR, West MS, Sloan M, et al. New Treatment Strategies for Metastatic Pancreatic Ductal Adenocarcinoma. *HHS Public Access.* 2020;80(7):647-669. doi:10.1007/s40265-020-01304-0.New
23. Mini E, Nobili S, Caciagli B, Landini I, Mazzei T. Cellular pharmacology of gemcitabine. *Ann Oncol.* 2006;17(Supplement 5):7-12. doi:10.1093/annonc/mdj941
24. Zeng S, Pöttler M, Lan B, Grützmann R, Pilarsky C, Yang H. Chemoresistance in pancreatic cancer. *Int J Mol Sci.* 2019. doi:10.3390/ijms20184504
25. Kamisawa T, Wood LD, Itoi T, Takaori K. Pancreatic cancer. *Lancet.* 2016;388(10039):73-85. doi:10.1016/S0140-6736(16)00141-0
26. Jia Y, Xie J. Promising molecular mechanisms responsible for gemcitabine resistance in cancer. *Genes Dis.* 2015;2(4):299-306. doi:10.1016/j.gendis.2015.07.003
27. Donadelli M, Costanzo C, Beghelli S, et al. Synergistic inhibition of pancreatic adenocarcinoma cell growth by trichostatin A and gemcitabine. *Biochim Biophys Acta - Mol Cell Res.* 2007;1773(7):1095-1106. doi:10.1016/j.bbamcr.2007.05.002



28. Donadelli M, Dando I, Pozza ED, Palmieri M. Mitochondrial uncoupling protein 2 and pancreatic cancer: A new potential target therapy. *World J Gastroenterol*. 2015. doi:10.3748/wjg.v21.i11.3232
29. Ju HQ, Gocho T, Aguilar M, et al. Mechanisms of overcoming intrinsic resistance to gemcitabine in pancreatic ductal adenocarcinoma through the redox modulation. *Mol Cancer Ther*. 2015;14(3):788-798. doi:10.1158/1535-7163.MCT-14-0420
30. Pan ST, Li ZL, He ZX, Qiu JX, Zhou SF. Molecular mechanisms for tumour resistance to chemotherapy. *Clin Exp Pharmacol Physiol*. 2016;43(8):723-737. doi:10.1111/1440-1681.12581
31. Amrutkar M. Stellate Cells Aid Growth-Permissive Metabolic. 2021:1-21.
32. Meng Q, Liang C, Hua J, et al. A miR-146a-5p/TRAF6/NF- $\kappa$ B p65 axis regulates pancreatic cancer chemoresistance: Functional validation and clinical significance. *Theranostics*. 2020;10(9):3967-3979. doi:10.7150/thno.40566
33. Domenichini A, Adamska A, Falasca M. ABC transporters as cancer drivers: Potential functions in cancer development. *Biochim Biophys Acta - Gen Subj*. 2019;1863(1):52-60. doi:10.1016/j.bbagen.2018.09.019
34. Protein Atlas Database. doi:10.1007/springerreference\_33237
35. Mohelnikova-Duchonova B, Brynychova V, Oliverius M, et al. Differences in transcript levels of ABC transporters between pancreatic adenocarcinoma and nonneoplastic tissues. *Pancreas*. 2013;42(4):707-716. doi:10.1097/MPA.0b013e318279b861
36. Belkahla S, Khan AUH, Gitenay D, et al. Changes in metabolism affect expression of ABC transporters through ERK5 and depending on p53 status. *Oncotarget*. 2018;9(1):1114-1129. doi:10.18632/oncotarget.23305
37. König J, Hartel M, Nies AT, et al. Expression and localization of human multidrug resistance protein (ABCC) family members in pancreatic carcinoma. *Int J Cancer*. 2005. doi:10.1002/ijc.20831
38. Kohan HG, Boroujerdi M. Time and concentration dependency of P-gp, MRP1 and MRP5 induction in response to gemcitabine uptake in Capan-2 pancreatic cancer cells. *Xenobiotica*. 2015. doi:10.3109/00498254.2014.1001809
39. Adema AD, Floor K, Smid K, et al. Overexpression of MRP4 (ABCC4) and MRP5 (ABCC5) confer resistance to the nucleoside analogs cytarabine and troxacitabine, but not gemcitabine. *Springerplus*. 2014;3(1):1-11. doi:10.1186/2193-1801-3-732

40. Haggmann W, Jesnowski R, Löhr JM. Interdependence of gemcitabine treatment, transporter expression, and resistance in human pancreatic carcinoma cells. *Neoplasia*. 2010. doi:10.1593/neo.10576
41. Amponsah PS, Fan P, Bauer N, et al. microRNA-210 overexpression inhibits tumor growth and potentially reverses gemcitabine resistance in pancreatic cancer. *Cancer Lett*. 2017;388(December):107-117. doi:10.1016/j.canlet.2016.11.035
42. Oguri T, Achiwa H, Sato S, et al. The determinants of sensitivity and acquired resistance to gemcitabine differ in non-small cell lung cancer: A role of ABCC5 in gemcitabine sensitivity. *Mol Cancer Ther*. 2006;5(7):1800-1806. doi:10.1158/1535-7163.MCT-06-0025
43. Nath S, Daneshvar K, Roy LD, et al. MUC1 induces drug resistance in pancreatic cancer cells via upregulation of multidrug resistance genes. *Oncogenesis*. 2013;2(6):e51-9. doi:10.1038/oncsis.2013.16
44. Li Y, Revalde JL, Reid G, Paxton JW. Modulatory effects of curcumin on multidrug resistance-associated protein 5 in pancreatic cancer cells. *Cancer Chemother Pharmacol*. 2011;68(3):603-610. doi:10.1007/s00280-010-1515-6
45. Taylor J, Bebawy M. Proteins Regulating Microvesicle Biogenesis and Multidrug Resistance in Cancer. *Proteomics*. 2019;19(1-2). doi:10.1002/pmic.201800165
46. Koundouros N, Poulgiannis G. Reprogramming of fatty acid metabolism in cancer. *Br J Cancer*. 2020;122(1):4-22. doi:10.1038/s41416-019-0650-z
47. Li Z, Sun C, Qin Z. Metabolic reprogramming of cancer-associated fibroblasts and its effect on cancer cell reprogramming. *Theranostics*. 2021;11(17):8322-8336. doi:10.7150/THNO.62378
48. Pisanti S, Picardi P, D'Alessandro A, Laezza C, Bifulco M. The endocannabinoid signaling system in cancer. *Trends Pharmacol Sci*. 2013;34(5):273-282. doi:10.1016/j.tips.2013.03.003
49. Natalya N. Pavlova and Craig B. Thompson. Emerging metabolic hallmarks of cancer. *Physiol Behav*. 2018;176(1):139-148. doi:10.1016/j.cmet.2015.12.006.THE
50. Santos CR, Schulze A. Lipid metabolism in cancer. *FEBS J*. 2012;279(15):2610-2623. doi:10.1111/j.1742-4658.2012.08644.x
51. Kuhajda FP. Synthesis and antitumor activity of an inhibitor of fatty acid synthase. *Proc Natl Acad Sci*. 2000;97(7):3450-3454. doi:10.1073/pnas.050582897
52. Tadros S, Shukla SK, King RJ, et al. De Novo lipid synthesis facilitates

- gemcitabine resistance through endoplasmic reticulum stress in pancreatic cancer. *Cancer Res.* 2017;77(20):5503-5517. doi:10.1158/0008-5472.CAN-16-3062
53. Li J, Qu X, Tian J, Zhang JT, Cheng JX. Cholesterol esterification inhibition and gemcitabine synergistically suppress pancreatic ductal adenocarcinoma proliferation. *PLoS One.* 2018;13(2):1-11. doi:10.1371/journal.pone.0193318
  54. Parrales A, Iwakuma T. p53 as a regulator of lipid metabolism in cancer. *Int J Mol Sci.* 2016. doi:10.3390/ijms17122074
  55. Kaoutari A El, Fraunhoffer NA, Hoare O, et al. Metabolomic profiling of pancreatic adenocarcinoma reveals key features driving clinical outcome and drug resistance. *EBioMedicine.* 2021;66:103332. doi:10.1016/j.ebiom.2021.103332
  56. Luo X, Cheng C, Tan Z, et al. Emerging roles of lipid metabolism in cancer metastasis. *Mol Cancer.* 2017;16(1):1-10. doi:10.1186/s12943-017-0646-3
  57. Kang JH, Ko HM, Han GD, et al. Dual role of phosphatidylserine and its receptors in osteoclastogenesis. *Cell Death Dis.* 2020;11(7). doi:10.1038/s41419-020-2712-9
  58. Szlaza W, Zendran I, Zalesińska A, Tarek M, Kulbacka J. Lipid composition of the cancer cell membrane. *J Bioenerg Biomembr.* 2020;52(5):321-342. doi:10.1007/s10863-020-09846-4
  59. Wang L, Zhu W, Zhao Y, et al. Monoacylglycerol lipase promotes progression of hepatocellular carcinoma via NF- $\kappa$ B-mediated epithelial-mesenchymal transition. *J Hematol Oncol.* 2016;9(1):1-13. doi:10.1186/s13045-016-0361-3
  60. Louie, S. M., Roberts, L. S., Mulvihill, M. M., Luo, K., & Nomura DK. Cancer Cells Incorporate and Remodel Exogenous Palmitate into Structural and Oncogenic Signaling Lipids. *Biochim Biophys Acta.* 2014;1831(10):1-16. doi:10.1016/j.bbailip.2013.07.008.Cancer
  61. Zhang J, Liu Z, Lian Z, et al. Monoacylglycerol Lipase: A Novel Potential Therapeutic Target and Prognostic Indicator for Hepatocellular Carcinoma. *Sci Rep.* 2016;6(September):1-13. doi:10.1038/srep35784
  62. Deng H, Li W. Monoacylglycerol lipase inhibitors: modulators for lipid metabolism in cancer malignancy, neurological and metabolic disorders. *Acta Pharm Sin B.* 2020;10(4):582-602. doi:10.1016/j.apsb.2019.10.006
  63. Carracedo A, Gironella M, Lorente M, et al. Cannabinoids induce apoptosis of pancreatic tumor cells via endoplasmic reticulum stress-related genes. *Cancer Res.* 2006;66(13):6748-6755. doi:10.1158/0008-5472.CAN-06-0169
  64. Donadelli M, Dando I, Zaniboni T, et al. Gemcitabine/cannabinoid combination

- triggers autophagy in pancreatic cancer cells through a ROS-mediated mechanism. *Cell Death Dis.* 2011;2(4):e152-12. doi:10.1038/cddis.2011.36
65. Laezza C, Pagano C, Navarra G, et al. The endocannabinoid system: A target for cancer treatment. *Int J Mol Sci.* 2020;21(3). doi:10.3390/ijms21030747
  66. Zhao H, Yang L, Baddour J, et al. Tumor microenvironment derived exosomes pleiotropically modulate cancer cell metabolism. *Elife.* 2016;5(FEBRUARY2016):1-27. doi:10.7554/eLife.10250
  67. Von Ahrens D, Bhagat TD, Nagrath D, Maitra A, Verma A. The role of stromal cancer-associated fibroblasts in pancreatic cancer. *J Hematol Oncol.* 2017;10(1):1-8. doi:10.1186/s13045-017-0448-5
  68. Narayanan S, Vicent S, Ponz-Sarvisé M. PDAC as an Immune Evasive Disease: Can 3D Model Systems Aid to Tackle This Clinical Problem? *Front Cell Dev Biol.* 2021;9(December):1-13. doi:10.3389/fcell.2021.787249
  69. Jaiswal R, Johnson MS, Pokharel D, Krishnan SR, Bebawy M. Microparticles shed from multidrug resistant breast cancer cells provide a parallel survival pathway through immune evasion. *BMC Cancer.* 2017;17(1):1-12. doi:10.1186/s12885-017-3102-2
  70. Orlandi A, Calegari MA, Martini M, et al. Gemcitabine versus FOLFIRINOX in patients with advanced pancreatic adenocarcinoma hENT1-positive: everything was not too bad back when everything seemed worse. *Clin Transl Oncol.* 2016;18(10):988-995. doi:10.1007/s12094-015-1471-z
  71. Nordh S, Ansari D, Andersson R. hENT1 expression is predictive of gemcitabine outcome in pancreatic cancer: A systematic review. *World J Gastroenterol.* 2014;20(26):8482-8490. doi:10.3748/wjg.v20.i26.8482
  72. Bird NTE, Elmasry M, Jones R, et al. Immunohistochemical hENT1 expression as a prognostic biomarker in patients with resected pancreatic ductal adenocarcinoma undergoing adjuvant gemcitabine-based chemotherapy. *Br J Surg.* 2017;104(4):328-336. doi:10.1002/bjs.10482
  73. Aughton K, Elander NO, Evans A, et al. HENT1 predicts benefit from gemcitabine in pancreatic cancer but only with low CDA mRNA. *Cancers (Basel).* 2021;13(22):5758. doi:10.3390/cancers13225758
  74. Shin DW, Lee J chan, Kim J, et al. Tailored adjuvant gemcitabine versus 5-fluorouracil/folinic acid based on hENT1 immunohistochemical staining in resected pancreatic ductal adenocarcinoma: A biomarker stratified prospective trial. *Pancreatology.* 2021;21(4):796-804. doi:10.1016/j.pan.2021.02.022

75. Grasso C, Jansen G, Giovannetti E. Drug resistance in pancreatic cancer: Impact of altered energy metabolism. *Crit Rev Oncol Hematol*. 2017;114:139-152. doi:10.1016/j.critrevonc.2017.03.026
76. Xi Y, Yuan P, Li T, Zhang M, Liu MF, Li B. hENT1 reverses chemoresistance by regulating glycolysis in pancreatic cancer. *Cancer Lett*. 2020;479(October 2019):112-122. doi:10.1016/j.canlet.2020.03.015
77. Sierzega M, Pach R, Kulig P, Legutko J, Kulig J. Prognostic implications of expression profiling for gemcitabine-related genes (hENT1, dCK, RRM1, RRM2) in patients with resectable pancreatic adenocarcinoma receiving adjuvant chemotherapy. *Pancreas*. 2017;46(5):684-689. doi:10.1097/MPA.0000000000000807
78. Lolkema P, Jodrell DI, Tuveson DA. nab-paclitaxel potentiates gemcitabine activity by reducing cytidine deaminase levels in a mouse model of pancreatic cancer. 2016;2(3):260-269. doi:10.1158/2159-8290.CD-11-0242.nab
79. Hessmann E, Patzak MS, Klein L, et al. Fibroblast drug scavenging increases intratumoural gemcitabine accumulation in murine pancreas cancer. *Gut*. 2018;67(3):497-507. doi:10.1136/gutjnl-2016-311954
80. Yoneyama H, Takizawa-Hashimoto A, Takeuchi O, et al. Acquired resistance to gemcitabine and cross-resistance in human pancreatic cancer clones. *Anticancer Drugs*. 2015;26(1):90-100. doi:10.1097/CAD.0000000000000165
81. Reid G, Wielinga P, Zelcer N, et al. Characterization of the transport of nucleoside analog drugs by the human multidrug resistance proteins MRP4 and MRP5. *Mol Pharmacol*. 2003;63(5):1094-1103. doi:10.1124/mol.63.5.1094
82. Bruckdorfer R. The basics about nitric oxide. *Mol Aspects Med*. 2005;26(1-2 SPEC. ISS.):3-31. doi:10.1016/j.mam.2004.09.002
83. Huang Z, Fu J, Zhang Y. Nitric Oxide Donor-Based Cancer Therapy: Advances and Prospects. *J Med Chem*. 2017. doi:10.1021/acs.jmedchem.6b01672
84. Celia H. ,Tengan; Carlos T. M. NO control of mitochondrial function in normal and transformed cells. *Physiol Behav*. 2018;176(5):139-148. doi:10.1016/j.bbabbio.2017.02.009.NO
85. Mintz J, Vedenko A, Rosete O, et al. Current advances of nitric oxide in cancer and anticancer therapeutics. *Vaccines*. 2021;9(2):1-39. doi:10.3390/vaccines9020094
86. Carpenter A, Schoenfisch M. Nitric Oxide Release Part II. Therapeutic Applications. *Chem Soc Rev*. 2012;41(10):3742-3752.

- doi:10.1039/c2cs15273h.Nitric
87. Seth D, Hess DT, Hausladen A, Wang L, Wang Y juan, Stamler JS. A Multiplex Enzymatic Machinery for Cellular Protein S-nitrosylation. *Mol Cell*. 2018. doi:10.1016/j.molcel.2017.12.025
  88. Bartesaghi S, Radi R. Fundamentals on the biochemistry of peroxynitrite and protein tyrosine nitration. *Redox Biol*. 2018;14(September):618-625. doi:10.1016/j.redox.2017.09.009
  89. Zhan X, Huang Y, Qian S. Protein Tyrosine Nitration in Lung Cancer: Current Research Status and Future Perspectives. *Curr Med Chem*. 2018;25(29):3435-3454. doi:10.2174/0929867325666180221140745
  90. Riganti C, Miraglia E, Viarisio D, et al. Nitric oxide reverts the resistance to doxorubicin in human colon cancer cells by inhibiting the drug efflux. *Cancer Res*. 2005. doi:65/2/516 [pii]
  91. Masetto F, Chegaev K, Gazzano E, et al. MRP5 nitration by NO-releasing gemcitabine encapsulated in liposomes confers sensitivity in chemoresistant pancreatic adenocarcinoma cells. *Biochim Biophys Acta - Mol Cell Res*. 2020. doi:10.1016/j.bbamcr.2020.118824
  92. Tuccinardi T, Granchi C, Rizzolio F, et al. Identification and characterization of a new reversible MAGL inhibitor. *Bioorganic Med Chem*. 2014;22(13):3285-3291. doi:10.1016/j.bmc.2014.04.057
  93. Ahn K, Johnson DS, Mileni M, et al. Discovery and Characterization of a Highly Selective FAAH Inhibitor that Reduces Inflammatory Pain. *Chem Biol*. 2009;16(4):411-420. doi:10.1016/j.chembiol.2009.02.013
  94. Vemuri S, Rhodes CT. Preparation and characterization of liposomes as therapeutic delivery systems: a review. *Pharm Acta Helv*. 1995;70(2):95-111. doi:10.1016/0031-6865(95)00010-7
  95. Massihnia D, Avan A, Funel N, et al. Phospho-Akt overexpression is prognostic and can be used to tailor the synergistic interaction of Akt inhibitors with gemcitabine in pancreatic cancer. *J Hematol Oncol*. 2017;10(1). doi:10.1186/s13045-016-0371-1
  96. Freyria FS, Bonelli B, Tomatis M, et al. Hematite nanoparticles larger than 90 nm show no sign of toxicity in terms of lactate dehydrogenase release, nitric oxide generation, apoptosis, and comet assay in murine alveolar macrophages and human lung epithelial cells. *Chem Res Toxicol*. 2012. doi:10.1021/tx2004294
  97. Chegaev K, Fraix A, Gazzano E, et al. Light-Regulated NO Release as a Novel

- Strategy To Overcome Doxorubicin Multidrug Resistance. *ACS Med Chem Lett.* 2017;8(3):361-365. doi:10.1021/acsmchemlett.7b00016
98. Firuzi O, Che PP, El Hassouni B, et al. Role of c-MET inhibitors in overcoming drug resistance in spheroid models of primary human pancreatic cancer and stellate cells. *Cancers (Basel)*. 2019. doi:10.3390/cancers11050638
  99. El Hassouni B, Mantini G, Li Petri G, et al. To Combine or Not Combine: Drug Interactions and Tools for Their Analysis. Reflections from the EORTC-PAMM Course on Preclinical and Early-phase Clinical Pharmacology. *Anticancer Res.* 2019;39(7):3303-3309. doi:10.21873/anticancerres.13472
  100. Desbats MA, Giacomini I, Prayer-Galetti T, Montopoli M. Metabolic Plasticity in Chemotherapy Resistance. *Front Oncol.* 2020;10(March). doi:10.3389/fonc.2020.00281
  101. Huerta S, Chilka S, Bonavida B. Nitric oxide donors: novel cancer therapeutics (review). *Int J Oncol.* 2008;33(5):909-927. <http://www.ncbi.nlm.nih.gov/pubmed/18949354>.
  102. Zeybek ND, Inan S, Ekerbicer N, Vatansever HS, Karakaya J, Muftuoglu SF. The effects of Gemcitabine and Vinorelbine on inducible nitric oxide synthase (iNOS) and endothelial nitric oxide synthase (eNOS) distribution of MCF-7 breast cancer cells. *Acta Histochem.* 2011. doi:10.1016/j.acthis.2009.07.006
  103. Yang J, Sontag D, Gong Y, Minuk GY. Enhanced gemcitabine cytotoxicity with knockdown of multidrug resistance protein genes in human cholangiocarcinoma cell lines. *J Gastroenterol Hepatol.* 2021;36(4):1103-1109. doi:10.1111/jgh.15289
  104. Guo H, Liu F, Yang S, Xue T. Emodin alleviates gemcitabine resistance in pancreatic cancer by inhibiting MDR1/P-glycoprotein and MRPs expression. *Oncol Lett.* 2020;20(5):1-7. doi:10.3892/OL.2020.12030
  105. De Boo S, Kopecka J, Brusa D, et al. iNOS activity is necessary for the cytotoxic and immunogenic effects of doxorubicin in human colon cancer cells. *Mol Cancer.* 2009. doi:10.1186/1476-4598-8-108
  106. Pedrini I, Gazzano E, Chegaev K, et al. Liposomal nitrooxy-doxorubicin: One step over Caelyx in drug-resistant human cancer cells. *Mol Pharm.* 2014. doi:10.1021/mp500257s
  107. Di Pietro N, Giardinelli A, Sirolli V, et al. Nitric oxide synthetic pathway and cGMP levels are altered in red blood cells from end-stage renal disease patients. *Mol Cell Biochem.* 2016. doi:10.1007/s11010-016-2723-0
  108. Tang Z, Li C, Kang B, Gao G, Li C, Zhang Z. GEPIA: a web server for cancer

- and normal gene expression profiling and interactive analyses. *Nucleic Acids Res.* 2017;45(W1):W98-W102. doi:10.1093/nar/gkx247
109. Avan A, Caretti V, Funel N, et al. Crizotinib Inhibits Metabolic Inactivation of Gemcitabine in c-Met–driven Pancreatic Carcinoma. *Cancer Res.* 2013;73(22):6745-6756. doi:10.1158/0008-5472.CAN-13-0837
  110. Long JZ, Li W, Booker L, et al. Selective blockade of 2-arachidonoylglycerol hydrolysis produces cannabinoid behavioral effects. *Nat Chem Biol.* 2009;5(1):37-44. doi:10.1038/nchembio.129
  111. Granchi C, Bononi G, Ferrisi R, et al. Design, synthesis and biological evaluation of second-generation benzoylpiperidine derivatives as reversible monoacylglycerol lipase (MAGL) inhibitors. *Eur J Med Chem.* 2021. doi:10.1016/j.ejmech.2020.112857
  112. Butera G, Brandi J, Cavallini C, et al. The mutant P53-driven secretome has oncogenic functions in pancreatic ductal adenocarcinoma cells. *Biomolecules.* 2020;10(6):1-21. doi:10.3390/biom10060884
  113. Fiorini C, Cordani M, Padroni C, Blandino G, Di Agostino S, Donadelli M. Mutant p53 stimulates chemoresistance of pancreatic adenocarcinoma cells to gemcitabine. *Biochim Biophys Acta - Mol Cell Res.* 2015. doi:10.1016/j.bbamcr.2014.10.003
  114. Seth Nanda C, Venkateswaran SV, Patani N, Yuneva M. Defining a metabolic landscape of tumours: genome meets metabolism. *Br J Cancer.* 2020;122(2):136-149. doi:10.1038/s41416-019-0663-7
  115. Fu Y, Zou T, Shen X, et al. Lipid metabolism in cancer progression and therapeutic strategies. *MedComm.* 2021;2(1):27-59. doi:10.1002/mco2.27
  116. Gnanamony M, Gondi CS. Chemoresistance in pancreatic cancer: Emerging concepts (Review). *Oncol Lett.* 2017;13(4):2507-2513. doi:10.3892/ol.2017.5777
  117. Du J, Gu J, Li J. Mechanisms of drug resistance of pancreatic ductal adenocarcinoma at different levels. *Biosci Rep.* 2020;40(7). doi:10.1042/BSR20200401
  118. Arpicco S, Battaglia L, Brusa P, et al. Recent studies on the delivery of hydrophilic drugs in nano- particulate systems. *J Drug Deliv Sci Technol.* 2015. doi:10.1016/j.jddst.2015.09.004.This
  119. Arpicco S, Lerda C, Dalla Pozza E, et al. Hyaluronic acid-coated liposomes for active targeting of gemcitabine. *Eur J Pharm Biopharm.* 2013;85(3 PART A):373-380. doi:10.1016/j.ejpb.2013.06.003



120. Bouillet P, Huang DCS, O'Reilly LA, et al. The role of the pro-apoptotic Bcl-2 family member bim in physiological cell death. *Ann N Y Acad Sci.* 2000;926:83-89. doi:10.1111/j.1749-6632.2000.tb05601.x
121. Dalla Pozza E, Fiorini C, Dando I, et al. Role of mitochondrial uncoupling protein 2 in cancer cell resistance to gemcitabine. *Biochim Biophys Acta - Mol Cell Res.* 2012. doi:10.1016/j.bbamcr.2012.06.007
122. Bian X, Liu R, Meng Y, Xing D, Xu D, Lu Z. Lipid metabolism and cancer. *J Exp Med.* 2021;218(1):1-17. doi:10.1084/JEM.20201606
123. Nomura DK, Long JZ, Niessen S, Hoover HS, Ng SW, Cravatt BF. Monoacylglycerol Lipase Regulates a Fatty Acid Network that Promotes Cancer Pathogenesis. *Cell.* 2010;140(1):49-61. doi:10.1016/j.cell.2009.11.027
124. Gil-Ordóñez A, Martín-Fontecha M, Ortega-Gutiérrez S, López-Rodríguez ML. Monoacylglycerol lipase (MAGL) as a promising therapeutic target. *Biochem Pharmacol.* 2018;157(July):18-32. doi:10.1016/j.bcp.2018.07.036
125. Bononi G, Tonarini G, Poli G, et al. Monoacylglycerol lipase (MAGL) inhibitors based on a diphenylsul fi de-benzoylpiperidine scaffold. *Eur J Med Chem.* 2021;223:113679. <https://doi.org/10.1016/j.ejmech.2021.113679>.
126. Bilimoria KY, Bentrem DJ, Ko CY, et al. Validation of the 6th edition AJCC pancreatic cancer staging system. *Cancer.* 2007;110(4):738-744. doi:10.1002/cncr.22852
127. Randazzo O, Papini F, Mantini G, et al. "Open Sesame?": Biomarker Status of the Human Equilibrative Nucleoside Transporter-1 and Molecular Mechanisms Influencing its Expression and Activity in the Uptake and Cytotoxicity of Gemcitabine in Pancreatic Cancer. *Cancers (Basel).* 2020;12(11):3206. doi:10.3390/cancers12113206
128. Funel N. The role of miR-21 and miR-211 on MMP9 regulation in pancreatic ductal adenocarcinoma: Cooperation in invasiveness behaviors? *Epigenomics.* 2015;7(3):333-335. doi:10.2217/epi.15.19
129. Jimenez RE, Hartwig W, Antoniu BA, Compton CC, Warshaw AL, Fernández-Del Castillo C. Effect of matrix metalloproteinase inhibition on pancreatic cancer invasion and metastasis: An additive strategy for cancer control. *Ann Surg.* 2000;231(5):644-654. doi:10.1097/00000658-200005000-00004
130. Blandino G, Levine AJ, Oren M. Mutant p53 gain of function: Differential effects of different p53 mutants on resistance of cultured cells to chemotherapy. *Oncogene.* 1999;18(2):477-485. doi:10.1038/sj.onc.1202314

131. Metabolism M, Queiroz AL, Smith D, Gimenez-cassina A. Effect of Mutant p53 Proteins on Glycolysis and Mitochondrial Metabolism. *Mol Cell Biol.* 2017;37(24):1-17.